Ecological Informatics 81 (2024) 102639

Contents lists available at ScienceDirect

Ecological Informatics

journal homepage: www.elsevier.com/locate/ecolinf

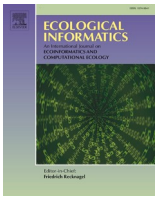

Computational modeling of animal behavior in T-mazes: Insights from machine learning

Ali Turab [a,d], Wutiphol Sintunavarat [b,*], Farhan Ullah [a], Shujaat Ali Zaidi [c], Andrés Montoyo [d,**], Josué-Antonio Nescolarde-Selva [e]

[a] School of Software, Northwestern Polytechnical University, 127 West Youyi Road, Beilin District, Xi'an 710072, China
[b] Department of Mathematics and Statistics, Faculty of Science and Technology, Thammasat University Rangsit Center, Pathum Thani 12120, Thailand
[c] Department of Computer Science, Faculty of Science, Chiang Mai University, Thailand
[d] Department of Software and Computing Systems, University of Alicante, Alicante, Spain
[e] Department of Applied Mathematics, University of Alicante, Alicante, Spain

ARTICLE INFO

MSC (2020):
92D50
00A71
68U07
91B06
47H10

Keywords:
Animal behavior
Decision-making
T-mazes
Computational modeling
Solution
Machine learning methods

ABSTRACT

This study investigates the intricacies of animal decision-making in T-maze environments through a synergistic approach combining computational modeling and machine learning techniques. Focusing on the binary decision-making process in T-mazes, we examine how animals navigate choices between two paths. Our research employs a mathematical model tailored to the decision-making behavior of fish, offering analytical insights into their complex behavioral patterns. To complement this, we apply advanced machine learning algorithms, specifically Support Vector Machines (SVM), K-Nearest Neighbors (KNN), and a hybrid approach involving Principal Component Analysis (PCA) for dimensionality reduction followed by SVM for classification to analyze behavioral data from zebrafish and rats. The above techniques result in high predictive accuracies, approximately 98.07% for zebrafish and 98.15% for rats, underscoring the efficacy of computational methods in decoding animal behavior in controlled experiments. This study not only deepens our understanding of animal cognitive processes but also showcases the pivotal role of computational modeling and machine learning in elucidating the dynamics of behavioral science.

1. Introduction

The study of animal decision-making has significantly evolved by incorporating high-resolution tracking systems and computational tools. These innovations have transformed our analysis of spatial navigation and decision-making within controlled environments, such as T-mazes, which offer a structured setting to scrutinize animal cognitive mechanisms (see (Deacon and Rawlins, 2006a; Deacon and Rawlins, 2006b; Sih et al., 2004)). While empirical data provides a foundational understanding of behavior, recent research integrates these observations with computational models to elucidate the complexities of decision-making (see (d'Isa et al., 2021; Ferrarini and Gustin, 2022; Wang, 2019)). The current study continues this interdisciplinary approach, combining machine learning and mathematical modeling to dissect the decision-making processes observed in T-maze experiments.

Furthermore, in behavioral ecology, animals navigate many decisions related to survival and reproduction, each reflecting the complex interaction between their internal states and external pressures. Investigating these decisions, from binary choices to complex, context-dependent ones, has expanded our comprehension of cognitive capacities, challenging preconceived notions of animal behavior (see (Johnson and Redish, 2007; Preuschoff et al., 2013; Tolman, 1948)). The fusion of mathematical modeling and machine learning in this research offers a dual advantage—enhancing the clarity and specificity of hypotheses while leveraging computational power to identify patterns in behavior, even in the face of data limitations (for more detail, see (Bhattacharjee et al., 2019; Collins and Shenhav, 2022; Valletta et al., 2017)).

Mathematical models demand precise hypothesis formulation, aiding in the clear differentiation and comparison of theoretical

* Corresponding author at: Department of Mathematics and Statistics, Faculty of Science and Technology, Thammasat University Rangsit Center, Pathum Thani 12120, Thailand.
** Correspondence to: A. Montoyo, Department of Software and Computing Systems, University of Alicante, Alicante, Spain.
E-mail addresses: wutiphol@mathstat.sci.tu.ac.th (W. Sintunavarat), montoyo@dlsi.ua.es (A. Montoyo).

https://doi.org/10.1016/j.ecoinf.2024.102639
Received 11 January 2024; Received in revised form 1 April 2024; Accepted 7 May 2024
Available online 11 May 2024

predictions. In contrast, machine learning, particularly neural networks, and deep learning provides powerful tools for pattern recognition, albeit with challenges in data requirements and interpretability (see (Barak and Tsodyks, 2023; Kliegr et al., 2020; Kuru et al., 2023; Tron and Margaliot, 2004; Vos et al., 2006)). By adopting an integrative approach, we not only maintain the interpretability of traditional models but also benefit from the predictive capabilities of machine learning, advancing our ability to predict behavioral outcomes in a wide range of scenarios. This methodology propels our investigation forward, opening new avenues for anticipating animal behavior in various conditions and emphasizing the controlled settings of T-maze experiments.

The central aim of this research is to demystify the complex decision-making processes of animals in controlled settings, with a particular focus on the T-maze environment. This study transcends traditional observational strategies, employing mathematical modeling as a pivotal tool to theoretically elucidate animal behaviors. By complementing this, the research harnesses the power of sophisticated machine learning techniques to scrutinize empirical data, as demonstrated by studying zebrafish and rat behaviors in the T-maze. By synergizing theoretical models with empirical analysis, this research endeavors to meld abstract mathematical principles with tangible behavioral patterns. This integrative approach provides a holistic perspective on the intricacies of animal decision-making, offering valuable insights into their cognitive processes.

This manuscript is meticulously organized to facilitate a coherent and progressive exploration of our research. The introductory section lays the groundwork, acquainting the reader with the study's objectives and significance. An extensive review of relevant literature follows it, situating our investigation within the broader scholarly discourse. The paper then progresses to a focused case study on paradise fish behavior within T-maze environments, applying our theoretical concepts practically. Subsequently, we delve into our mathematical model's theoretical underpinnings and analytical rigor, offering a deep dive into its foundational aspects and computational intricacies. The subsequent section is dedicated to a detailed examination of zebrafish and rat behaviors in T-mazes, employing SVM, KNN, and PCA-SVM methods for detailed analysis. The paper culminates with a conclusive section that not only encapsulates our key findings but also charts potential directions for future research endeavors, thereby extending the scope of our study beyond its current horizons.

2. Literature review

Making choices is an integral part of behavior in all animal species. Deciding entails pinpointing and opting for a singular physiological, behavioral, or cognitive pathway among various possibilities. This intricate process requires the amalgamation of varied informational inputs and the reconciliation of competing demands. A key characteristic of decision-making is the inherent uncertainty about the consequences of the selected path. As such, overt or covert decision-making necessitates an organism's ability to forecast the most beneficial course of action. The capacity for prediction is vital across all life forms, playing a critical role in their survival and evolutionary adaptation. Intriguingly, this faculty for anticipatory decision-making is not limited to complex organisms; even single-celled microorganisms demonstrate this ability in their behavioral patterns and in maintaining internal equilibrium (for more detail, see (Balázsi et al., 2011; Bleuven and Landry, 2016; Lyon, 2015)).

The spontaneous alternation T-maze stands as a cornerstone in assessing spatial working memory. This T-shaped structure offers a bifurcation, presenting two divergent paths. Its origins trace back to the early 1910s, conceived by Robert Yerkes at Harvard University, initially for probing the cognitive capabilities and learning behaviors of invertebrates, particularly earthworms (Yerkes, 1912). In the subsequent decade, Edward Tolman adapted this apparatus for exploring rodent cognition, thereby pioneering the observation of what is known as spontaneous alternation (Tolman, 1925). Further refinement and exploration of this phenomenon were undertaken in the 1930s by Wayne Dennis (Dennis, 1935; Dennis and Henneman, 1932; Dennis and Sollenberger, 1934), who also introduced the term "spontaneous alternation" (Dennis, 1939).

Fundamentally, the spontaneous alternation T-maze capitalizes on rodents' innate penchant for novelty, prompting them to alternate their exploratory choices between the maze's arms (see (Deacon and Rawlins, 2006a; Dember and Richman, 2012; Montgomery, 1952; Tolman, 1925)). Such inclinations, which emerge naturally without needing prior training and stem from rodents' attraction to novel stimuli, have been labeled spontaneous. An alternate hypothesis posits that this behavior might be an inherent tendency in mice to alternate their choices, driven by outcomes such as finding or not finding food, leading to win-shift or lose-shift behaviors, respectively. In either scenario, whether driven by novelty-seeking or innate shifting tendencies, the animal must recall the previously visited arm to successfully alternate choices. This makes the spontaneous alternation T-maze a robust tool for evaluating spatial working memory.

Over the last century, the application of spontaneous alternation has extended beyond rodents to a diverse array of mammalian species, including rats (Tolman, 1925), mice (Henderson, 1970), hamsters (Kirkby and Lackey, 1968), guinea pigs (Douglas et al., 1973), rabbits (Hughes, 1973), gerbils (Dember and Kleinman, 1973), ferrets (Hughes, 1965), opossums (Tilley et al., 1966), marmosets (Izumi et al., 2013), and cats (Frederickson and Frederickson, 1979). Remarkably, this behavior has also been observed in various non-mammalian species, such as pill bugs (Shokaku et al., 2020), garden woodlice (Hughes, 1967), marine crabs (Ramey et al., 2009), fruit flies (Lewis et al., 2017; May and Wellman, 1968), goldfish (Fidura and Leberer, 1974), and zebrafish (Cognato et al., 2012), underscoring its utility in a broad spectrum of cognitive research across different taxa.

In animal behavior studies, the integration of Machine Learning (ML) and Deep Learning (DL) methodologies represents a significant paradigm shift. Traditionally, these advanced computational techniques, renowned for their predictive accuracy in fields such as artificial intelligence (Marar, 2024), image processing (Zhang et al., 2015), neuroscience (Dixon and Polson, 2020), and genomics (Xiao and Segal, 2009), have not been extensively harnessed for modeling or predicting animal movement. Such approaches extend the application of these technologies beyond their conventional domains and aim to transcend the mere prediction of behavior. The objective is to craft a methodology that utilizes machine learning to forecast behavioral patterns and intricately map animals' actual movement trajectories.

This endeavor necessitates a departure from traditional parametric models commonly used in animal movement studies, which have predominantly focused on deciphering patterns and timings of animal movements through state space models like Hidden Markov Models (HMMs), step selection function models, and resource selection models. These conventional models, while effective, often rely on deterministic or stochastic approaches, limiting their scope in capturing the full complexity of animal behavior. In contrast, integrating ML and DL offers a more comprehensive understanding, bridging the gap between predictive modeling and the intricate dynamics of animal behavior in natural habitats. The strength of this integrated approach lies in its ability to encapsulate the known properties of a system through mathematical or physical representations, thereby reducing reliance on teleological explanations. By differentiating between rational, mathematical models, which are grounded in fundamental theories, and empirical models, which fit specific data without a theoretical basis, this study aims to enhance scientific understanding significantly. The rational models, whether deterministic or stochastic, provide a robust framework for understanding the nature of animal behavior, whether governed by chance or predictability, thus offering a more profound insight into the behavioral dynamics of animals in their environments (for more detail, see (Browning et al., 2018; Calenge et al., 2009; Nazir and Kaleem,

2021)).

On the other hand, Epstein introduced a model (Epstein, 1966) to describe the learning behaviors of animals across multiple events, articulated as follows

$$\mathbf{P}(x+\alpha)-\mathbf{P}(x)=e^{-x}\{\mathbf{P}(x)-\mathbf{P}(x-\beta)\} \tag{2.1}$$

where a and b represent positive constants, while $\mathbf{P}(x)$ signifies the probability of absorption for each value of x, necessitating that the inequalities $0 \leq \mathbf{P}(x) \leq 1$ are satisfied. The defined boundary conditions are $\mathbf{P}(-\infty)=0$ and $\mathbf{P}(+\infty)=1$. It is important to note that $\mathbf{P}$ is not considered a cumulative distribution function, and thus, its monotonicity is not a prerequisite. Nonetheless, it was demonstrated that a unique bounded function fulfilling eq. (2.1) with the specified boundary conditions at $\pm\infty$ exists. The solution exhibits monotonicity, ensuring compliance with the inequalities $0 \leq \mathbf{P}(x) \leq 1$.

Later on, Istrăţescu discussed the existence of a unique solution for a functional Eq. (Istrăţescu, 1976) designed to model the decision-making process of predatory animals when presented with multiple choices

$$\mathbf{P}(x)=x\mathbf{P}((1-\alpha)x+\alpha)+(1-x)\mathbf{P}((1-\beta)x) \tag{2.2}$$

where $0<\alpha \leq \beta<1$ and $\mathbf{P}$ denote a continuous function defined over the interval $[0,1]$. On the other hand, Lubič and Shapiro, leveraging the profound Schauder fixed point theorem, established the existence of a solution for the above eq. (2.2) under the following conditions (see (Istrăţescu, 1976))

$$\begin{aligned}&\mathbf{P}_0(x)=\sum_{i=1}^{\infty} a_i x^i, \quad a_i \geqslant 0,\\ &\mathbf{P}_0(0)=0, \quad \mathbf{P}_0(1)=1.\end{aligned} \tag{2.3}$$

In (Turab and Sintunavarat, 2019), the authors investigated the decision-making behavior of paradise fish within a T-maze configuration formulating the subsequent functional equation to model this process

$$\mathbf{P}(x)=x\mathbf{P}(\alpha_1 x+1-\alpha_1)+(1-x)\mathbf{P}(\alpha_2 x) \tag{2.4}$$

for all $x \in [0,1]$, where $\mathbf{P}:[0,1]\to\mathbb{R}$ is an unknown function such that $\mathbf{P}(0)=0$, $\mathbf{P}(1)=1$ and $0<\alpha_1 \leq \alpha_2<1$. They used the fixed point results to obtain the existence and uniqueness of a solution to the functional eq. (2.4).

Turab and Sintunavarat expanded the previous work by introducing the following novel functional equation to model a specific type of learning behavior (see (Turab and Sintunavarat, 2020))

$$\mathbf{P}(x)=x\mathbf{P}(\alpha_1 x+(1-\alpha_1)\lambda_1)+(1-x)\mathbf{P}(\alpha_2 x+(1-\alpha_2)\lambda_2) \tag{2.5}$$

for every $x \in [0,1]$, where $\mathbf{P}:[0,1]\to\mathbb{R}$ represents an unknown function, $0<\alpha_1 \leq \alpha_2<1$, and both λ_1, λ_2 lie within the interval $[0,1]$. The functional eq. (2.5) models the phenomenon of emotional resilience observed in a controlled experimental setup, involving a small enclosure with a steel grid floor, designed to study learning behaviors in dogs.

Subsequent research into human and animal behavior within the context of probabilistic learning theory has yielded numerous results in this area of study (see (Debnath, 2021; George et al., 2022; Schein, 1954; Turab et al., 2022a; Turab et al., 2022b; Turab et al., 2023; Turab and Sintunavarat, 2023)).

3. Movement of a paradise fish in a T-maze: A case study

Reflecting on the seminal work of Bush and Wilson (Bush and Wilson, 1956), this section delves into the intricacies of paradise fish behavior within a T-maze setup, a pivotal study in animal behavior research. The experiment presented paradise fish with a binary navigational choice in a T-maze: to swim either towards the right or left at the tank's far end. Notably, one path, designated as the beneficial side, consistently offered a reward of caviar 75% of the time, in contrast to the alternative path's 25% reward frequency. This experimental design yielded four distinct outcomes: right reward, left reward, right non-reward, and left non-reward.

They hypothesized that receiving a reward on one side would likely increase the fish's preference for that side in subsequent trials. However, the response to non-rewarded trials introduced a theoretical divergence. While information or extinction theory suggested a decreased probability of selecting the non-rewarded side again, habit formation or secondary reinforcement theory proposed that any visit to a side would increase its selection likelihood in the future. Their mathematical model encapsulated this theoretical dichotomy, adjusting the probability of side selection based on trial outcomes.

Assuming p represents the probability of a fish selecting the right-hand side of a tank if rewarded for such a choice, the likelihood of choosing the right side in subsequent trials increases. Bush and Wilson suggested that the updated probability for opting for the right side follows the formula $\alpha_1 p+1-\alpha_1$, where α_1, a learning parameter, falls between 0 and 1. For instance, with $p=0.4$ and $\alpha_1=0.8$, the updated probability calculates to 0.52. Similarly, it is hypothesized that rewards for selecting the left side would also adjust the probability of future right-side choices, albeit more modestly.

Consistency within the experiment presupposes identical learning rates for choices on both sides. The model posits that the probability of choosing the right decreases by $\alpha_1 p$ in the face of non-reinforcement, embodying a theory of extinction. Conversely, the model predicts a minor increase in probability, $\alpha_2 p+1-\alpha_2$ (where α_2 is a learning parameter), for rewarded behavior, illustrating the concept of habit formation or secondary reinforcement. These theoretical predictions are delineated in Table 1, emphasizing the algebraic distinction between $\alpha_1 p$ and $\alpha_1 p+1-\alpha_1$ based on the perspective of right-turn probability rather than the direct influence of the last choice made.

Furthering their investigation, Bush and Wilson examined the impact of different divider conditions in the T-maze: an opaque divider obscuring the unrewarded goal box and a transparent one allowing visibility of the reward in the alternate box. This aspect of the experiment added a layer of complexity to the fish's decision-making process, mainly when the fish were aware of but unable to access a visible reward. The analysis of data from the last 49 trials across two groups of fish and the 22 simulated fish (referred to as 'stat-fish', a method for comparing model predictions with empirical data through Monte Carlo simulations, as described in (Alvarez, 2021)), as depicted in Fig. 1, reveals a marked preference for one side. This observation contests the reinforcement-extinction model's expectation of a balanced distribution around a median, suggesting the real fish behavior diverges significantly from the model's predictions. This finding underscores the efficacy of stochastic models in differentiating theoretical positions and enriching our understanding of animal behavior in controlled settings.

3.1. Statistical insights from the paradise fish experiment

In (Bush and Wilson, 1956), Bush and Wilson presented a statistical comparison between an experimental group of 22 real fish and a corresponding group of 22 stat-fish. The analysis includes the mean and standard deviation (SD) of the total number of runs, the frequency of runs of varying lengths, and the number of successful outcomes per subject (S).

Table 1
Operators for choice experiments.

	Left	Right
For reinforcement-extinction model (p = Prob)		
• Reinforcement	$\alpha_1 p$	$\alpha_1 p+1-\alpha_1$
• Non-reinforcement	$\alpha_2 p+1-\alpha_2$	$\alpha_2 p$
For habit formation model		
• Reinforcement	$\alpha_1 p$	$\alpha_1 p+1-\alpha_1$
• Non-reinforcement	$\alpha_2 p$	$\alpha_2 p+1-\alpha_2$

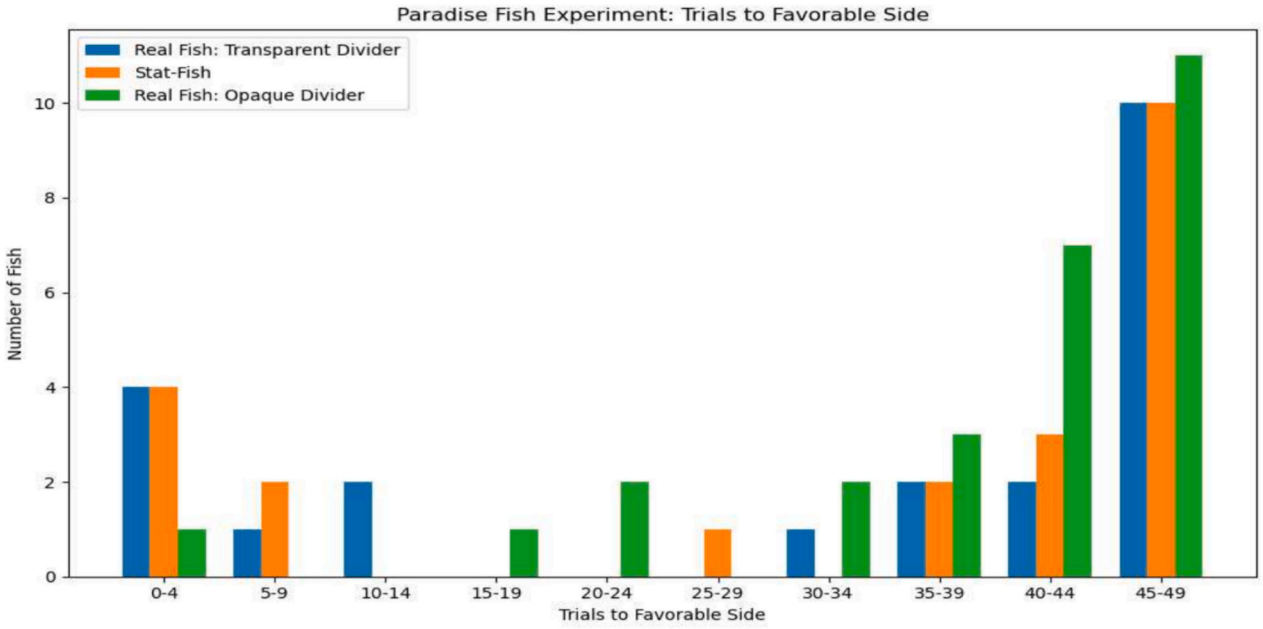

Fig. 1. Comparative analysis of paradise fish choices in T-maze trials.

In comparing the mean behaviors between the experimental group and stat-fish, it is observed that both groups exhibit similar trends across various run lengths, though stat-fish often show slightly higher means, particularly in the total number of runs and runs of length 1 (see Fig. 2). This pattern suggests that stat-fish might engage in shorter runs more frequently than the experimental group. Furthermore, the standard deviation values, indicative of behavioral variability, are consistently higher for stat-fish across most metrics (see Fig. 3 below). This increased variability hints at a less consistent behavioral pattern among stat-fish, possibly reflecting broader individual differences or varied responses to the experimental conditions.

The observed discrepancies likely stem from the behavior of certain stat-fish that rarely chose the unfavorable side. This contrasted with the real fish, where the minimum number of failures was five, suggesting that a less extreme initial probability distribution might have yielded closer alignment between the two groups. The symmetric beta distribution used in the stat-fish computations, serving as an approximation, might have yet to fully capture the initial variability in the real fish's behavior. The learning process during the initial trials suggests that the actual initial distribution of response probabilities for the real fish was likely broader than that used for the stat-fish.

3.2. *Conceptualizing decision-making processes in T-maze experiments*

Building upon Bush and Wilson's experimental design, Fig. 4 presents a conceptual representation of the decision-making process of animals in a T-maze experiment. The figure illustrates the initial position of the animal at the entrance of the T-maze, leading to a critical decision

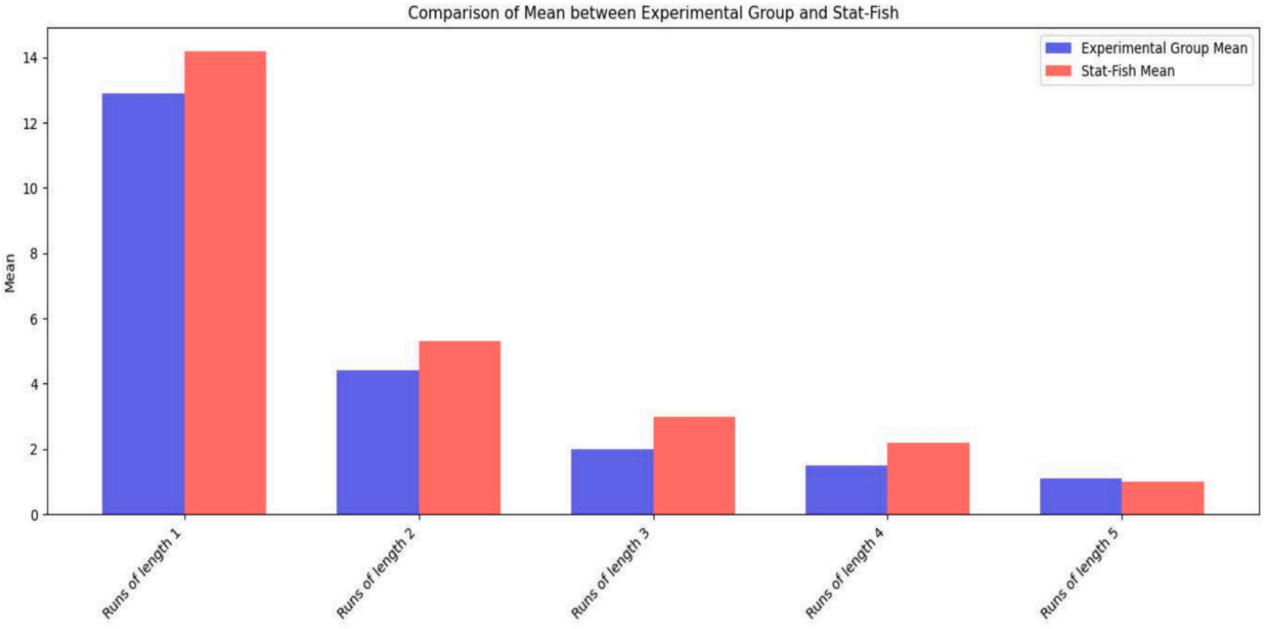

Fig. 2. Comparison of mean between experimental group and stat-fish.

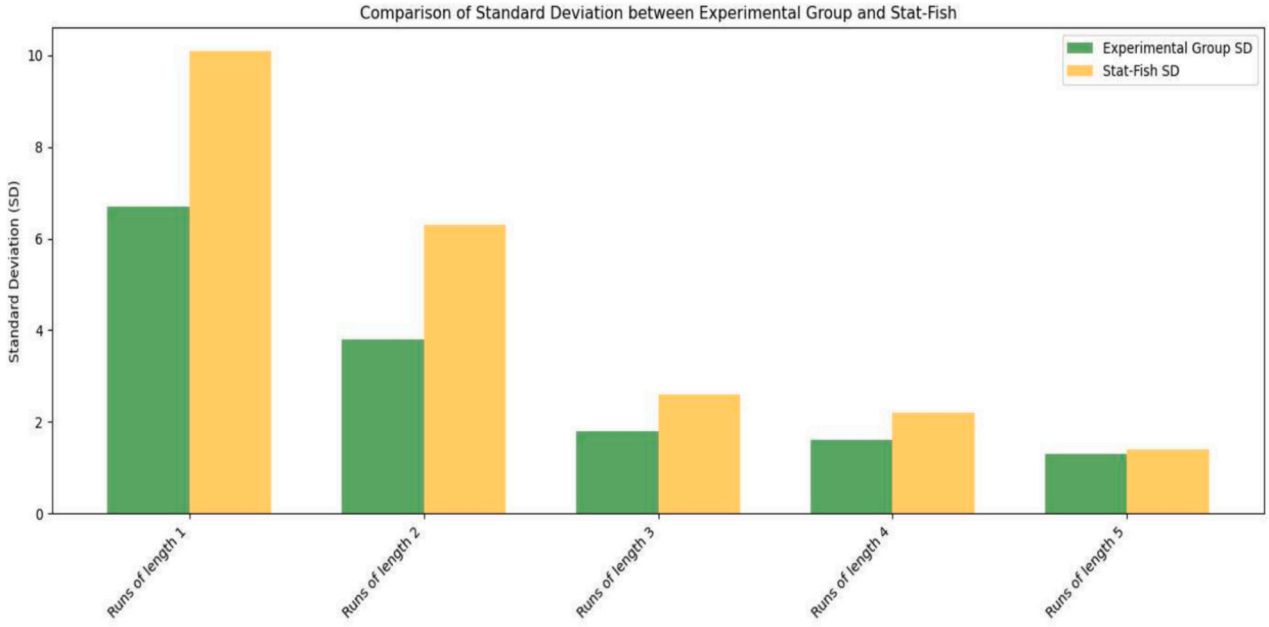

Fig. 3. Comparison of standard deviation between experimental group and stat-fish.

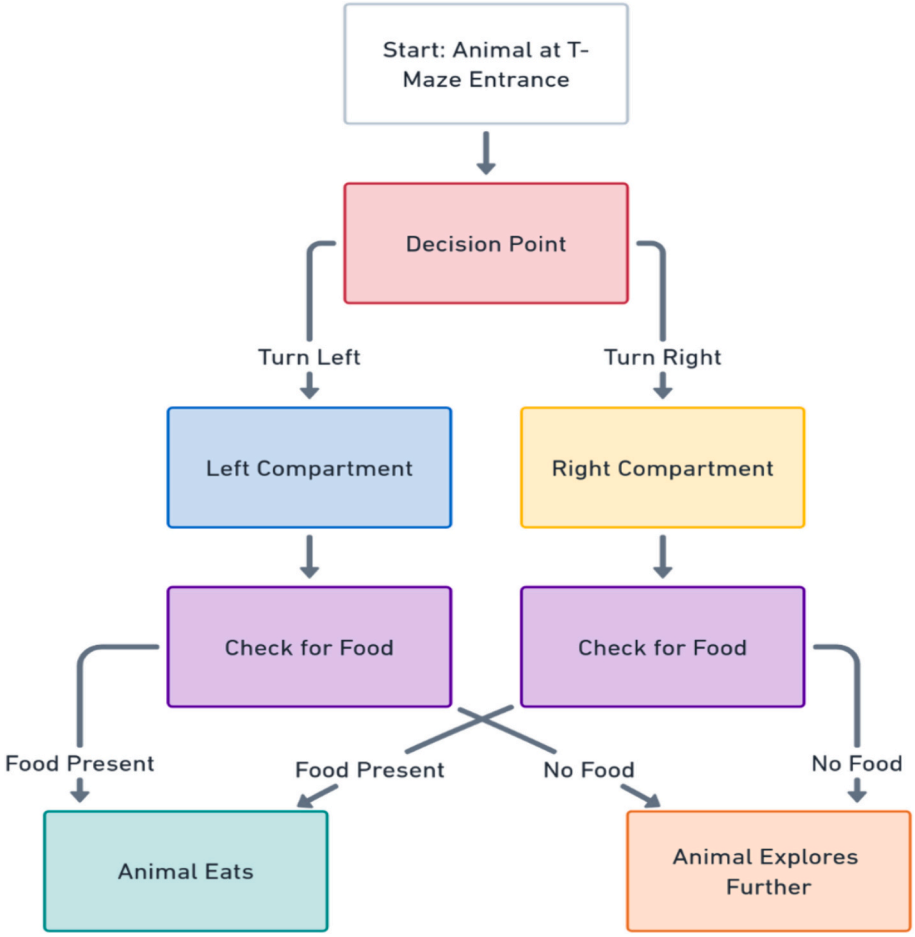

Fig. 4. Animal decision-making in T-maze: food location impact.

point where the animal must choose between turning left or right. Each path leads to a separate compartment – the left or right compartment – where the presence or absence of food is a crucial variable. The decision-making process is depicted as a series of binary choices, reflecting the animal's innate behavior in response to the environmental cues provided within the maze.

Upon reaching a compartment, the animal engages in a search behavior, represented by the decision node 'check for food.' If food is discovered, the outcome is denoted as 'animal eats,' indicating a successful foraging behavior. Conversely, if no food is present, the animal exhibits exploratory behavior, labeled 'animal explores further.' This exploration suggests the animal's adaptive response to the absence of an expected reward. This framework effectively encapsulates the essence of spatial decision-making in animals subjected to a T-maze setup. It highlights the influence of environmental factors, such as food placement, on their behavioral choices. The simplicity of the T-maze design, coupled with the complexity of the decision-making process, offers valuable insights into the cognitive mechanisms underlying animal behavior in controlled experimental settings.

4. Theoretical analysis and analytical investigations

4.1. Foundational mathematical concepts

Certain foundational results and mathematical structures are essential for developing our model. We begin by defining key properties of mappings within a metric space, as these properties are crucial for understanding our model's dynamics.

Definition 4.1 (Berinde and Takens, 2007)**.** *Let $(\mathbb{X}, d)$ be a metric space. An operator $\boldsymbol{P} : \mathbb{X} \to \mathbb{X}$ is characterized as follows:*

1. An θ-Lipschitzian mapping if it satisfies the inequality

$$d(\boldsymbol{P}\mu, \boldsymbol{P}\nu) \leq \theta d(\mu, \nu), \ \forall \mu, \nu \in \mathbb{X}, \ \text{where } \theta > 0; \tag{4.1}$$

2. *An κ-contraction mapping if $\boldsymbol{P}$ is κ-Lipschitzian, with $\kappa \in [0, 1)$;*
3. *A nonexpansive mapping if $\boldsymbol{P}$ is 1-Lipschitzian;*
4. *A contractive mapping if it fulfills the condition*

$$d(\boldsymbol{P}\mu, \boldsymbol{P}\nu) < d(\mu, \nu), \ \forall \mu, \nu \in \mathbb{X} \text{ with } \mu \neq \nu. \tag{4.2}$$

Building upon these definitions, we invoke a fundamental theorem in fixed-point theory, which is pivotal for our model's convergence analysis.

Theorem 4.1 (Banach, 1922). *Consider $(\mathbb{X}, d)$ as a complete metric space where an operator $\boldsymbol{P} : \mathbb{X} \to \mathbb{X}$ satisfies condition (2) of Definition 4.1. It is established that $\boldsymbol{P}$ possesses a unique fixed point $y^\star$, and for any $y \in \mathbb{X}$, the iterates of $\boldsymbol{P}$ converge to $y^\star$,* i.e.*,*

$$\boldsymbol{P}^n(y) \to y^\star \ \ (\text{as } n \to \infty).$$

These preliminary concepts and results lay the groundwork for our subsequent analysis, providing the mathematical underpinning for the rigorous study of decision-making processes in a T-maze setup.

4.2. Model formulation

In the formulation of our model, we define the state space as $\mathbb{X} = [0, 1]$ and denote $\mathscr{C}$ as the collection of all real-valued continuous functions $\mathbf{P} : \mathbb{X} \to \mathbb{R}$ that satisfy the following conditions:

$$\sup_{\mu \neq \nu} \frac{|\mathbf{P}(\mu) - \mathbf{P}(\nu)|}{|\mu - \nu|} < \infty, \text{ and } \mathbf{P}(0) = 0.$$

Here, $(\mathscr{C}, \|\cdot\|)$ constitutes a normed space, where the norm $\|\cdot\|$ is defined as:

$$\|\mathbf{P}\| = \sup_{\mu \neq \nu} \frac{|\mathbf{P}(\mu) - \mathbf{P}(\nu)|}{|\mu - \nu|}, \ \forall \mathbf{P} \in \mathscr{C}. \tag{4.3}$$

To encapsulate the decision-making process of an animal in a T-maze, we consider the following functional equation:

$$\mathbf{P}(x) = \mathrm{f}(x)\mathbf{P}(\mathscr{V}_1(x)) + (1 - \mathrm{f}(x))\mathbf{P}(\mathscr{V}_2(x)), \tag{4.4}$$

where $\mathscr{V}_1, \mathscr{V}_2 : \mathbb{X} \to \mathbb{X}$, $\forall x \in \mathbb{X}$, are mappings that satisfy the contraction condition with parameters ℓ_1 and ℓ_2, respectively, and $\mathscr{V}_2(0) = 0$ and $\mathbf{P} : \mathbb{X} \to \mathbb{R}$ is an unknown function. Moreover, $\mathrm{f} : \mathbb{X} \to \mathbb{X}$ is a nonexpansive mapping with $\mathrm{f}(0) = 0$ and $|\mathrm{f}(x)| \ \leq \ell_4$ ($\ell_4 \geq 0$), for all $x \in \mathbb{X}$.

In the context of analyzing the movement of paradise fish within a T-maze setup, as discussed in (Bush and Wilson, 1956), the parameters delineated in the functional eq. (4.4) are elucidated as follows:

1. **State space $\mathbb{X} = [0, 1]$:** This denotes the continuum of states, where each state $x \in \mathbb{X}$ symbolizes a probabilistic inclination towards choosing a specific direction (either left or right) within the T-maze.
2. **Learning rate functions $\mathscr{V}_1(x)$ and $\mathscr{V}_2(x)$:** These functions articulate the algebraic expressions for the learning rate parameters associated with the choices of left and right directions, respectively, by the paradise fish. They model the evolution of preference as the fish learns from its environment.
3. **Decision probability function $\mathrm{f}(x)$:** The function $\mathrm{f}(x)$, alongside its complement $(1 - \mathrm{f}(x))$, quantifies the probability distribution between the two available choices (left or right). This probabilistic behavior is encapsulated within a Markov process framework, where the state space $\mathbb{X} = [0, 1]$ represents all possible decision probabilities. The transition probabilities from any given state x to the subsequent states $\mathscr{V}_1(x)$ and $\mathscr{V}_2(x)$ are defined as:

$$\begin{aligned} &\mathrm{Prob}(x \to \mathscr{V}_1(x)) = \mathrm{f}(x), \\ &\mathrm{Prob}(x \to \mathscr{V}_2(x)) = 1 - \mathrm{f}(x), \end{aligned}$$

respectively, delineating the likelihood of transitioning towards each choice based on the current state.

4. **Outcome probability function P:** This function signifies the eventual probability of the fish consistently opting for a particular choice, predicated on the initial probability x of that choice being selected. It essentially models the culmination of the decision-making process, reflecting the fish's final preference after a series of choices.

4.3. Analytical solution

In this subsection, we delve into the analytical resolution of the decision-making model as delineated in eq. (4.4). The ensuing theorems and corollaries are instrumental in establishing the existence and uniqueness of solutions within the confines of our model framework. These results hinge on the intricate interplay between the mappings $\mathscr{V}_1$ and $\mathscr{V}_2$, and the probabilistic function $\mathrm{f}(x)$, which collectively orchestrate the decision-making process in our T-maze setup.

Theorem 4.2. *Consider the model* (4.4)*. Let*

$$|\mathscr{V}_1(\mu) - \mathscr{V}_2(\nu)| \leq \ell_3 |\mu - \nu|, \tag{4.5}$$

where $\ell_3 \in [0, 1)$, $\forall \mu, \nu \in \mathbb{X}$ with $\mu \neq \nu$, such that $\Xi_1 := [(1 + \ell_4)\ell_1 + \ell_2 + \ell_3] < 1$, and there exists a subset $\mathscr{E} \neq 0$ of $\mathscr{S} := \{\boldsymbol{P} \in \mathscr{C} | \boldsymbol{P}(1) \leq 1\}$ with the structure $(\mathscr{E}, \|\cdot\|)$ of a Banach space (given in (4.3)*). Then, a singular solution exists for the model* (4.4)*. Additionally, the sequence $\{\boldsymbol{P}_n\}$ converges to a unique solution of* (4.4)*, where $\boldsymbol{P}_0 \in \mathscr{E}$ and*

$$\boldsymbol{P}_n(x) = \mathrm{f}(x)\boldsymbol{P}_{n-1}(\mathscr{V}_1(x)) + (1 - \mathrm{f}(x))\boldsymbol{P}_{n-1}(\mathscr{V}_2(x)), \ \forall n \in \mathbb{N}.$$

Proof. Consider the complete metric space $(\mathscr{E}, d)$ induced by $\|\cdot\|$. Define an operator Φ on $\mathscr{E}$ as follows:

$$(\Phi\mathbf{P})(x) = \mathrm{f}(x)\mathbf{P}(\mathscr{V}_1(x)) + (1 - \mathrm{f}(x))\mathbf{P}(\mathscr{V}_2(x)), \ \forall x \in \mathbb{X}, \ \forall \mathbf{P} \in \mathscr{E}.$$

For each $\mathbf{P} \in \mathscr{E}$, it is evident that $(\Phi\mathbf{P})(0) = 0$. Since $\Phi\mathbf{P}$ is continuous and $\|\Phi\mathbf{P}\| < \infty$ for all $\mathbf{P} \in \mathscr{E}$, the operator $\Phi : \mathscr{E} \to \mathscr{E}$ is well-defined. Moreover, the fixed point of Φ corresponds to the solution of (4.4).

Given that $\Phi : \mathscr{E} \to \mathscr{E}$ is linear, for $\mathbf{P}_1, \mathbf{P}_2 \in \mathscr{E}$, we have

$$\|\Phi\mathbf{P}_1 - \Phi\mathbf{P}_2\| = \|\Phi(\mathbf{P}_1 - \mathbf{P}_2)\|.$$

To evaluate $\|\Phi\mathbf{P}_1 - \Phi\mathbf{P}_2\|$, consider:

$$\Theta_{\iota,\varsigma} := \frac{\Phi(\mathbf{P}_1 - \mathbf{P}_2)(\iota) - \Phi(\mathbf{P}_1 - \mathbf{P}_2)(\varsigma)}{\iota - \varsigma}, \forall \iota, \varsigma \in \mathbb{X}, \iota \neq \varsigma.$$

For $\iota, \varsigma \in \mathbb{X}$ with $\iota \neq \varsigma$, we derive

$$\begin{aligned}\Omega_{\iota,\varsigma} &= \frac{1}{\iota - \varsigma}\Big[\mathrm{f}(\iota)(P_1 - P_2)(V_1(\iota)) + (1 - \mathrm{f}(\iota))(P_1 - P_2)(V_2(\iota)) \\ &\quad -\mathrm{f}(\varsigma)(P_1 - P_2)(V_1(\varsigma)) - (1 - \mathrm{f}(\varsigma))(P_1 - P_2)(V_2(\varsigma))\Big] \\ &= \frac{1}{\iota - \varsigma}\Big[\mathrm{f}(\iota)(P_1 - P_2)(V_1(\iota)) - \mathrm{f}(\iota)(P_1 - P_2)(V_1(\varsigma)) \\ &\quad +(1 - \mathrm{f}(\iota))(P_1 - P_2)(V_2(\iota)) - (1 - \mathrm{f}(\iota))(P_1 - P_2)(V_2(\varsigma)) \\ &\quad +\mathrm{f}(\iota)(P_1 - P_2)(V_1(\varsigma)) - \mathrm{f}(\varsigma)(P_1 - P_2)(V_1(\varsigma)) \\ &\quad +(1 - \mathrm{f}(\iota))(P_1 - P_2)(V_2(\varsigma)) - (1 - \mathrm{f}(\varsigma))(P_1 - P_2)(V_2(\varsigma))\Big].\end{aligned}$$

Thus by (4.3), for $\iota, \varsigma \in \mathbb{X}$ with $\iota \neq \varsigma$, we have

$$\begin{aligned}|\Omega_{\iota,\varsigma}| \leq\ & |\mathrm{f}(\iota)|\frac{|(P_1 - P_2)(V_1(\iota)) - (P_1 - P_2)(V_1(\varsigma))|}{|V_1(\iota) - V_1(\varsigma)|}\frac{|V_1(\iota) - V_1(\varsigma)|}{|\iota - \varsigma|} \\ &+|1 - \mathrm{f}(\iota)|\frac{|(P_1 - P_2)(V_2(\iota)) - (P_1 - P_2)(V_2(\varsigma))|}{|V_2(\iota) - V_2(\varsigma)|}\frac{|V_2(\iota) - V_2(\varsigma)|}{|\iota - \varsigma|} \\ &+\frac{|(P_1 - P_2)(V_1(\varsigma)) - (P_1 - P_2)(V_1(\iota))|}{|V_1(\varsigma) - V_1(\iota)|}|V_1(\varsigma) - V_1(\iota)| \\ &+\frac{|(P_1 - P_2)(V_1(\iota)) - (P_1 - P_2)(V_2(\varsigma))|}{|V_1(\iota) - V_2(\varsigma)|}|V_1(\iota) - V_2(\varsigma)|.\end{aligned}$$

This yields that

$$\begin{aligned}|\Omega_{\iota,\varsigma}| &\leq (\ell_1|\mathrm{f}(\iota)| + \ell_2|1 - \mathrm{f}(\iota)| + \ell_1|\varsigma - \iota| + \ell_3|\iota - \varsigma|)\|V_1(\iota) - V_2(\varsigma)\| \\ &\leq \Xi_1\|V_1(\iota) - V_2(\varsigma)\|\end{aligned}$$

implying that

$$\begin{aligned}d(\Phi\mathbf{P}_1, \Phi\mathbf{P}_2) &= \|\Phi\mathbf{P}_1 - \Phi\mathbf{P}_2\| \\ &\leq \Xi_1\|\mathbf{P}_1 - \mathbf{P}_2\| \\ &= \Xi_1 d(\mathbf{P}_1, \mathbf{P}_2).\end{aligned}$$

Since $\Xi_1 < 1$, Theorem 4.1 ensures the existence of a singular solution for the model (4.4).

Now, we focus on a particular application of the previously established theorem. Specifically, we consider the scenario where the mappings $\mathscr{V}_1$ and $\mathscr{V}_2$ from $\mathbb{X}$ to $\mathbb{X}$ satisfy the condition (2) of Definition 4.1 with parameters ℓ_1 and ℓ_2, respectively, and where $\ell_1 \leq \ell_2$. Under these conditions, the following result, derived from Theorem 4.2, elucidates the existence and convergence of solutions within our decision-making model (4.4).

Corollary 4.1. *Consider the decision-making model as defined in* (4.4). *Let the inequality*

$$|\mathscr{V}_1(\mu) - \mathscr{V}_2(\nu)| \leq \ell_3|\mu - \nu|, \tag{4.6}$$

hold, where $\ell_3 \in [0, 1)$, $\forall \mu, \nu \in \mathbb{X}$ *with* $\mu \neq \nu$. *Assume that* $\Xi_1^\star := [(2 + \ell_4)\ell_2 + \ell_3] < 1$. *Furthermore, let there exist a non-empty subset* $\mathscr{E}$ *of* $\mathscr{S} := \{\mathbf{P} \in \mathscr{C} | \mathbf{P}(1) \leq 1\}$ *that forms a Banach space with the structure* $(\mathscr{E}, \|\cdot\|)$ *as defined in* (4.3). *Under these conditions, a singular solution exists for the model* (4.4). *Moreover, the sequence* $\{\mathbf{P}_n\}$, *where* $\mathbf{P}_0 \in \mathscr{E}$, *converges to a unique solution of* (4.4), *defined for each* $n \in \mathbb{N}$ *as*

$$\mathbf{P}_n(x) = \mathrm{f}(x)\mathbf{P}_{n-1}(\mathscr{V}_1(x)) + (1 - \mathrm{f}(x))\mathbf{P}_{n-1}(\mathscr{V}_2(x)).$$

The model (4.4) is now examined under diverse scenarios to ascertain the existence and convergence of a unique solution.

Theorem 4.3. *Consider the decision-making model as defined in* (4.4). *Assume that* $\Xi_2 := [(1 + \ell_4)\ell_1 + 2\ell_2] < 1$, *and there exists a point* $\xi \in [0, 1]$ *for which* $\mathscr{V}_1(\xi) = \mathscr{V}_2(\xi)$. *Additionally, let there be a non-empty subset* $\mathscr{E}$ *of* $\mathscr{S} := \{\mathbf{P} \in \mathscr{C} | \mathbf{P}(1) \leq 1\}$ *that forms a Banach space with the structure* $(\mathscr{E}, \|\cdot\|)$ *as specified in* (4.3). *Under these conditions, a singular solution exists for the model* (4.4). *Moreover, the sequence* $\{\mathbf{P}_n\}$, *where* $\mathbf{P}_0 \in \mathscr{E}$, *converges to a singular solution of* (4.4), *defined for each* $n \in \mathbb{N}$ *as*

$$\mathbf{P}_n(x) = \mathrm{f}(x)\mathbf{P}_{n-1}(\mathscr{V}_1(x)) + (1 - \mathrm{f}(x))\mathbf{P}_{n-1}(\mathscr{V}_2(x)).$$

Proof. The proof of Theorem 4.3 parallels that of Theorem 4.2, with emphasis on the differing elements. For each pair $\iota, \varsigma \in \mathbb{X}$, where $\iota \neq \varsigma$, the following expression is derived

$$\begin{aligned}\Omega_{\iota,\varsigma} &= \frac{1}{\iota - \varsigma}\Big[\mathrm{f}(\iota)(P_1 - P_2)(V_1(\iota)) + (1 - \mathrm{f}(\iota))(P_1 - P_2)(V_2(\iota)) \\ &\quad -\mathrm{f}(\varsigma)(P_1 - P_2)(V_1(\varsigma)) - (1 - \mathrm{f}(\varsigma))(P_1 - P_2)(V_2(\varsigma))\Big] \\ &= \frac{1}{\iota - \varsigma}\Big[\mathrm{f}(\iota)(P_1 - P_2)(V_1(\iota)) - \mathrm{f}(\iota)(P_1 - P_2)(V_1(\varsigma)) \\ &\quad +(1 - \mathrm{f}(\iota))(P_1 - P_2)(V_2(\iota)) - (1 - \mathrm{f}(\iota))(P_1 - P_2)(V_2(\varsigma)) \\ &\quad +\mathrm{f}(\iota)(P_1 - P_2)(V_1(\varsigma)) - \mathrm{f}(\varsigma)(P_1 - P_2)(V_1(\varsigma)) \\ &\quad +(1 - \mathrm{f}(\iota))(P_1 - P_2)(V_2(\varsigma)) - (1 - \mathrm{f}(\varsigma))(P_1 - P_2)(V_2(\varsigma))\Big].\end{aligned}$$

Thus by (4.3), for $\iota, \varsigma \in \mathbb{X}$ with $\iota \neq \varsigma$, we have

$$\begin{aligned}|\Omega_{\iota,\varsigma}| \leq\ & |\mathrm{f}(\iota)|\frac{|(P_1 - P_2)(V_1(\iota)) - (P_1 - P_2)(V_1(\varsigma))|}{|V_1(\iota) - V_1(\varsigma)|}\frac{|V_1(\iota) - V_1(\varsigma)|}{|\iota - \varsigma|} \\ &+|1 - \mathrm{f}(\iota)|\frac{|(P_1 - P_2)(V_2(\iota)) - (P_1 - P_2)(V_2(\varsigma))|}{|V_2(\iota) - V_2(\varsigma)|}\frac{|V_2(\iota) - V_2(\varsigma)|}{|\iota - \varsigma|} \\ &+\frac{|(P_1 - P_2)(V_1(\varsigma)) - (P_1 - P_2)(V_1(\xi))|}{|V_1(\varsigma) - V_1(\xi)|}|V_1(\varsigma) - V_1(\xi)| \\ &+\frac{|(P_1 - P_2)(V_2(\xi)) - (P_1 - P_2)(V_2(\varsigma))|}{|V_2(\xi) - V_2(\varsigma)|}|V_2(\xi) - V_2(\varsigma)|.\end{aligned} \tag{4.7}$$

The proof then considers two distinct cases:

Case 1. If $\xi = \varsigma$, the following inequality is established

$$\begin{aligned}|\Theta_{\iota,\varsigma}| &\leq (\ell_1|\mathrm{f}(\iota)| + \ell_2|1 - \mathrm{f}(\iota)|)\|\mathscr{V}_1(\iota) - \mathscr{V}_2(\varsigma)\| \\ &\leq \Xi_2\|\mathbf{P}_1 - \mathbf{P}_2\|.\end{aligned}$$

Case 2. If $\xi \neq \varsigma$, the inequality (4.7) becomes

$$\begin{aligned}|\Theta_{\iota,\varsigma}| &\leq (\ell_1|\mathrm{f}(\iota)| + \ell_2|1 - \mathrm{f}(\iota)| + \ell_1|\varsigma - \iota| + \ell_2|\iota - \varsigma|)\|V_1(\iota) - V_2(\varsigma)\| \\ &= \Xi_2\|V_1(\iota) - V_2(\varsigma)\|.\end{aligned}$$

This leads to the conclusion that the operator $\mathbf{P}$ is a contraction, and by Theorem 4.1, a unique solution exists for the model (4.4).

Corollary 4.2. *Consider the decision-making model as defined in eq.* (4.4). *Let the mappings* $\mathscr{V}_1, \mathscr{V}_2 : \mathbb{X} \to \mathbb{X}$ *satisfy the condition* (2) *of Definition* 4.1 *with parameters* ℓ_1 *and* ℓ_2, *respectively, ensuring that* $\ell_1 \leq \ell_2$. *Furthermore, assume that* $\Xi_2^\star := (3 + \ell_4)\ell_2 < 1$, *and there exists a point* $\xi \in [0, 1]$ *for which* $\mathscr{V}_1(\xi) = \mathscr{V}_2(\xi)$. *Additionally, let there be a non-empty subset* $\mathscr{E}$ *of the space* $\mathscr{S} := \{\mathbf{P} \in \mathscr{C} | \mathbf{P}(1) \leq 1\}$, *which forms a Banach space with the structure* $(\mathscr{E}, \|\cdot\|)$ *as defined in* (4.3)). *Under these conditions, a singular solution exists for the model* (4.4). *Moreover, the sequence* $\{\mathbf{P}_n\}$, *starting from any* $\mathbf{P}_0$ *in* $\mathscr{E}$, *converges to a unique solution of the model* (4.4). *The iterative process for this convergence is given by*:

$$\mathbf{P}_n(x) = \mathrm{f}(x)\mathbf{P}_{n-1}(\mathscr{V}_1(x)) + (1 - \mathrm{f}(x))\mathbf{P}_{n-1}(\mathscr{V}_2(x)), \forall n \in \mathbb{N}.$$

4.4. Convergence analysis

The study of convergence in iterative systems is pivotal across various fields, such as computer science and mathematics, where it

ensures system stability and solution reliability, signifying an algorithm's capacity to reach a solution consistently. In mathematical psychology, convergence takes on a unique meaning, relating to stabilizing learning or decision-making processes, and is crucial for understanding evolving learning patterns and cognitive processes. Within our study, convergence analysis of various iterative processes, detailed in Table 2, plays a crucial role in understanding decision-making dynamics in animals within the T-maze setup, highlighting these methods' unique characteristics and applications in our mathematical model.

The iteration processes detailed in the Table 2 are driven by terms like κ_n and ξ_n, and parameters such as $\overline{\lambda}$, all chosen within the $(0,1)$ range, and for the sequences $\{\mu_n\}_{n\in\mathbb{N}}$, $\{\nu_n\}_{n\in\mathbb{N}}$, $\{\omega_n\}_{n\in\mathbb{N}}$, $\{\widetilde{z}_n\}_{n\in\mathbb{N}}$, and $\{\tau_n\}_{n\in\mathbb{N}}$, respectively.

In our investigation, we discuss the Picard–Krasnoselskii hybrid iterative process, which demonstrates a more rapid convergence rate as compared to traditional methods such as the Picard iterative process, Mann iterative process, Krasnoselskii iterative process, and Ishikawa iterative process. This enhanced efficiency in reaching convergence underscores the effectiveness of the hybrid approach in complex decision-making models like the one explored in our study.

Theorem 4.4 (Okeke and Abbas, 2017). *Let $\mathscr{C}$ be a normed space and $\overline{\mathscr{A}}$ be a nonempty closed convex subset of $\mathscr{C}$ and $\mathscr{W}:\mathscr{C}\to\mathscr{C}$ be a contraction mapping (defined in Definition 4.1). Assume that each of the iteration processes defined in Table 2 converges to the same fixed point $\Xi^\star$ of $\mathscr{W}$, where $\{\kappa_n\}$ and $\{\xi_n\}$ are appropriately chosen sequences in $(0,1)$ such that $0<\overline{\kappa}\le\overline{\lambda},\kappa_n,\xi_n<1$ for all $n\in\mathbb{N}$ and for some $\overline{\kappa}$. Then the Picard–Krasnoselskii hybrid iterative process converges faster than all the other four processes.*

Now, we prove the results given in section 4 using the Picard-Krasnoselskii hybrid iterative process.

Theorem 4.5. Under the assumptions of Theorem 4.2, the proposed functional eq. (4.4) has a unique solution, say $\mathbf{P}^\star\in\mathscr{E}$, and the Picard–Krasnoselskii hybrid iterative sequence $\{\tau_n\}$, defined in Table 2, converges strongly to $\mathbf{P}^\star$.

Proof. Let $\{\tau_n\}$ be an iterative sequence defined in Picard–Krasnoselskii hybrid iterative process for the the operator Φ from $\mathscr{E}$ given by

$$(\Phi\mathbf{P})(x)=\mathrm{f}(x)\mathbf{P}(\mathscr{V}_1(x))+(1-\mathrm{f}(x))\mathbf{P}(\mathscr{V}_2(x)),\ \forall x\in\mathbb{X}\ \text{and}\ \forall\mathbf{P}\in\mathscr{E}.$$

Here, our aim is to prove that $\tau_n\to\mathbf{P}^\star$ as $n\to\infty$. For this, we need to compute

$$\begin{aligned}\|\tau_n-\mathbf{P}^\star\| &= \|\Phi\vartheta_n-\Phi\mathbf{P}^\star\|=\|\Phi(\vartheta_n-\mathbf{P}^\star)\|\\ &= \sup_{\iota\neq\varsigma}\frac{|\Phi(\vartheta_n-\mathbf{P}^\star)(\iota)-\Phi(\vartheta_n-\mathbf{P}^\star)(\varsigma)|}{|\iota-\varsigma|}.\end{aligned}$$

For each $\iota,\varsigma\in\mathbb{X}$ with $\iota\neq\varsigma$, we get

$$|\Omega_{\iota,\varsigma}|=\frac{|\Phi(\vartheta_n-\mathbf{P}^\star)(\iota)-\Phi(\vartheta_n-\mathbf{P}^\star)(\varsigma)|}{|\iota-\varsigma|}.$$

The line of the proof of this theorem is identical to that of Theorem 4.2. So, by following the steps mentioned in Theorem 4.2, we obtain

$$\|\tau_n-\mathbf{P}^\star\|\le\Xi_1\|\vartheta_n-\mathbf{P}^\star\|. \tag{4.8}$$

Furthermore

$$\begin{aligned}\|\vartheta_n-P^\star\| &= \left\|\left(1-\overline{\lambda}\right)\tau_n+\overline{\lambda}\Phi\tau_n-P^\star\right\|\\ &\le \left(1-\overline{\lambda}\right)\|\tau_n-P^\star\|+\overline{\lambda}\|\Phi\tau_n-\Phi P^\star\|\\ &\le \left(1-\overline{\lambda}\right)\|\tau_n-P^\star\|+\overline{\lambda}\sup_{\iota\neq\varsigma}\frac{|\Phi(\tau_n-P^\star)(\iota)-\Phi(\tau_n-P^\star)(\varsigma)|}{|\iota-\varsigma|}\\ &\le \left(1-\overline{\lambda}\right)\|\tau_n-P^\star\|+\overline{\lambda}\Xi_1\|\tau_n-P^\star\|\\ &= \widetilde{\Xi}\|\tau_n-P^\star\|,\end{aligned} \tag{4.9}$$

where $\widetilde{\Xi}:=\left(1-(1-\Xi_1)\overline{\lambda}\right)$.

From (4.8) and (4.9), we have

$$\begin{aligned}\|\tau_n-P^\star\| &\le \widetilde{\Xi}\|\tau_n-P^\star\|\\ &\vdots\\ &\le \widetilde{\Xi}^n\|\tau_n-P^\star\|.\end{aligned}$$

As $\widetilde{\Xi}<1$, therefore $lim_{n\to\infty}\|\tau_n-\mathbf{P}^\star\|=0$, which completes the proof.

4.5. Stability analysis

A pivotal question emerges in mathematical computation: Under what conditions can an approximate solution be considered effectively equivalent to the exact solution, especially in functional equations? We explore the viability of solutions that marginally diverge from specific equations as acceptable approximations. This inquiry extends to examine the stability of our proposed model (referenced in eq. (4.4)), where stability signifies the model's resilience to minor perturbations. A stable model ensures that slight inaccuracies in inputs do not cause significant output discrepancies, highlighting the model's reliability and robustness, with further insights available in seminal works (Aoki, 1950; Hyers, 1941; Hyers et al., 2012; Rassias, 1978; Ulam, 2012).

Theorem 4.6. *If Theorem 4.3 holds, the equation $\Phi\boldsymbol{P}=\boldsymbol{P}$, where $\Phi:\mathscr{C}\to\mathscr{C}$ by*

$$(\Phi\boldsymbol{P})(x)=\mathrm{f}(x)\boldsymbol{P}(\mathscr{V}_1(x))+(1-\mathrm{f}(x))\boldsymbol{P}(\mathscr{V}_2(x)), \tag{4.10}$$

satisfies the property of Hyers-Ulam-Rassias stability given in (Hyers et al., 2012) with $\alpha>0$, $\forall\,\mathbf{P}\in\mathscr{C}$ and $\forall x\in\mathbb{X}$.

Proof. Let $\mathbf{P}\in\mathscr{C}$ with $d(\Phi\mathbf{P},\mathbf{P})\le\varphi(\mathbf{P})$. By Theorem 4.3, there is a unique $\mathbf{P}^\star\in\mathscr{C}$ having the property $\Phi\mathbf{P}^\star=\mathbf{P}^\star$. Thus, we get

$$\begin{aligned}d(\mathbf{P},\mathbf{P}^\star) &\le d(\mathbf{P},\mathbf{P}\Phi)+d(\mathbf{P}\Phi,\mathbf{P}^\star)\\ &\le \varphi(\mathbf{P})+d(\mathbf{P}\Phi,\Phi\mathbf{P}^\star)\\ &\le \varphi(\mathbf{P})+\Xi_2 d(\mathbf{P},\mathbf{P}^\star),\end{aligned}$$

where Ξ_2 is given in Theorem 4.3, and so

$$d(\mathbf{P},\mathbf{P}^\star)\le\alpha\varphi(\mathbf{P}),\ \textit{with}\ \alpha:=(1-\Xi_2)^{-1}.$$

The subsequent outcome regarding Hyers-Ulam stability is obtained based on the above analysis.

Corollary 4.3. *If Theorem 4.3 holds, the equation $\Phi\boldsymbol{P}=\boldsymbol{P}$, where $\Phi:\mathscr{C}\to\mathscr{C}$ defined as*

$$(\Phi\boldsymbol{P})(x)=\mathrm{f}(x)\boldsymbol{P}(\mathscr{V}_1(x))+(1-\mathrm{f}(x))\boldsymbol{P}(\mathscr{V}_2(x)), \tag{4.11}$$

has Hyers-Ulam stability given in (Hyers et al., 2012) with $\beta>0$,

Table 2
Summary of some iterative processes.

Iterative Process	Definition	Reference
Picard iterative process	$\mu_1=\mu\in\overline{\mathscr{A}}$, $\mu_{n+1}=\mathscr{W}\mu_n,\quad n\in\mathbb{N}$	(Picard, 1890)
Mann iterative process	$\nu_1=\nu\in\overline{\mathscr{A}}$, $\nu_{n+1}=(1-\kappa_n)\nu_n+\kappa_n\mathscr{W}\nu_n,\quad n\in\mathbb{N}$	(Mann, 1953)
Krasnoselskii iterative process	$\omega_1=\omega\in\overline{\mathscr{A}}$, $\omega_{n+1}=\left(1-\overline{\lambda}\right)\omega_n+\overline{\lambda}\mathscr{W}\omega_n,\quad n\in\mathbb{N}$	(Xiang and Yuan, 2015)
Ishikawa iterative process	$\widetilde{z}_1=\widetilde{z}\in\overline{\mathscr{A}}$, $\widetilde{z}_{n+1}=(1-\kappa_n)\widetilde{z}_n+\kappa_n\mathscr{W}\widetilde{y}_n$, $\widetilde{y}_n=(1-\xi_n)\widetilde{z}_n+\xi_n\mathscr{W}\widetilde{z}_n,\quad n\in\mathbb{N}$	(Ishikawa, 1974)
Picard-Krasnoselskii hybrid process	$\tau_1=\tau\in\overline{\mathscr{A}}$, $\tau_{n+1}=\mathscr{W}\vartheta_n$, $\vartheta_n=\left(1-\overline{\lambda}\right)\tau_n+\overline{\lambda}\mathscr{W}\tau_n,\quad n\in\mathbb{N}$	(Okeke and Abbas, 2017)

$\forall \boldsymbol{P} \in \mathscr{C}$ and $\forall \boldsymbol{x} \in \mathbb{X}$.

5. Behavioral dynamics in T-mazes: Zebrafish and rat movements

This section discusses our methods and designs for analyzing animal behavior in T-maze setups, focusing on zebrafish and rats. We describe our experimental setup, data acquisition, and use of machine learning to interpret movement patterns, providing insight into these species' decision-making processes in controlled environments.

5.1. Methodology and design

In our research, we embarked on a comprehensive exploration of the behavioral dynamics of zebrafish and rats within a T-maze environment. The core of our methodology revolved around a meticulously designed T-maze setup tailored to elicit and capture the decision-making processes of these animals. The data for the movements of zebrafish and rats within the T-maze setup can be obtained from (Benvenutti et al., 2021; Liu et al., 2023; Lucon-Xiccato and Bisazza, 2017; Yang and Mailman, 2018) and the references therein.We employed advanced machine learning methods to study and analyze the movement trajectories of zebrafish and rats in the T-maze setup. We focused on the centroid points of the movements, which laid the groundwork for our computational analysis.

Intriguing insights into species-specific navigational strategies are evident in Figs. 5–8, depicting the movement trajectories within a T-maze framework. Zebrafish exhibit notable variability and frequent direction changes, particularly on the left side of the maze (Fig. 5). This behavior can reflect a trial-and-error approach or the influence of less developed spatial memory. In contrast, rat trajectories are more streamlined and targeted, especially when navigating to the right side (Fig. 7), suggesting a more refined cognitive map or higher learning efficiency. Despite these differences, both organisms exhibit common behavioral pauses at the original centroids, potentially indicating critical decision points or cognitive processing zones within the maze. These pauses can point to a shared underlying navigational mechanism across species. The contrast in movement patterns highlights potential differences in how zebrafish and rats process spatial information, evaluate options, and execute decisions, providing valuable insights for comparative cognitive research.

5.2. Statistical analysis of movement patterns

The statistical analysis of the centroid coordinates from the T-maze experiments provided significant insights into the movement patterns of both zebrafish and rats. For zebrafish, the mean vectors for left and right movements were computed as $\mu_{\text{left}} = (242.82, 150.12)$ and $\mu_{\text{right}} = (291.54, 106.04)$, respectively. These vectors indicate a notable lateral displacement, particularly in leftward movements. The standard deviations, $\sigma_{\text{left}} = (23.83, 39.28)$ and $\sigma_{\text{right}} = (19.09, 51.17)$, suggest greater variability along the y-axis in rightward movements. The *t*-test results, with a statistic of $[-24.72, 11.00]$ and a *p*-value of $[2.73 \times 10^{-89}, 2.10 \times 10^{-25}]$, statistically validate the non-randomness in the movement patterns, indicating a significant directional bias in the zebrafish's navigational choices.

In the rat T-maze experiment, the mean centroid coordinates for leftward and rightward movements were $(142.45, 92.95)$ and $(318.67, 140.50)$, respectively. The standard deviations, 80.71 and 83.27 for leftward movements and 78.54 and 103.35 for rightward movements, highlight a significant spread in the positional data. The t-test statistics, -38.29 for the horizontal axis and -9.00 for the vertical axis, along with *p*-values of 1.35×10^{-213} and 7.82×10^{-19}, confirm the statistical significance of these findings. This analysis not only demonstrates distinct spatial preferences in the rats' decision-making but also emphasizes the effectiveness of centroid point analysis in understanding the complex spatial dynamics of animal behavior in controlled experiments.

5.3. Results and discussion

5.3.1. Computational configuration and hyperparameter settings

This study employed Jupyter Notebook 6.5.4 with a Python 3 IPython kernel to implement KNN, SVM, and a hybrid PCA-SVM method. Key libraries such as numpy, matplotlib, opencv, pandas, and scikit-learn were utilized for the extensive machine learning algorithms, data preprocessing, and model evaluation capabilities. The following hyperparameters were used:

1. For KNN
   - The determination of the optimal number of neighbors ('2-neighbors') was achieved through cross-validation, employing grid

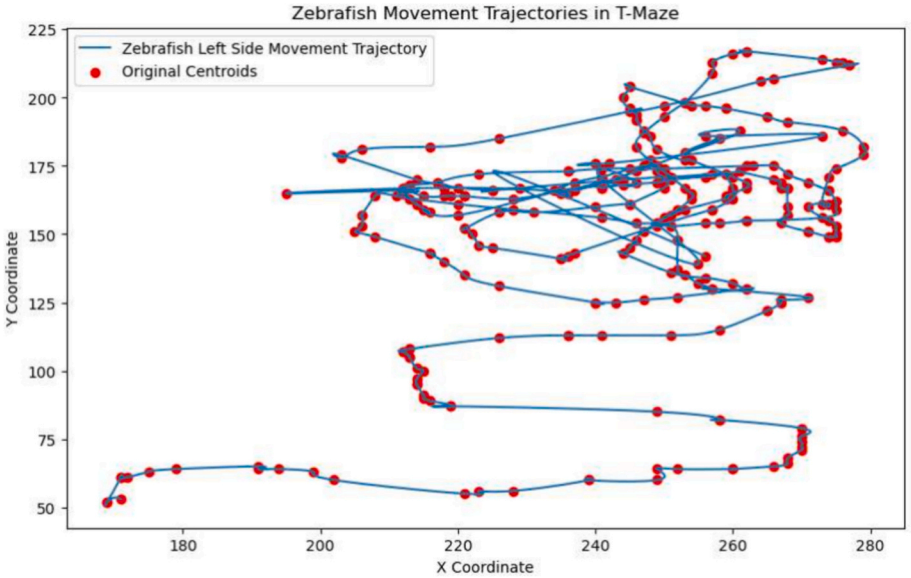

Fig. 5. Left movement.

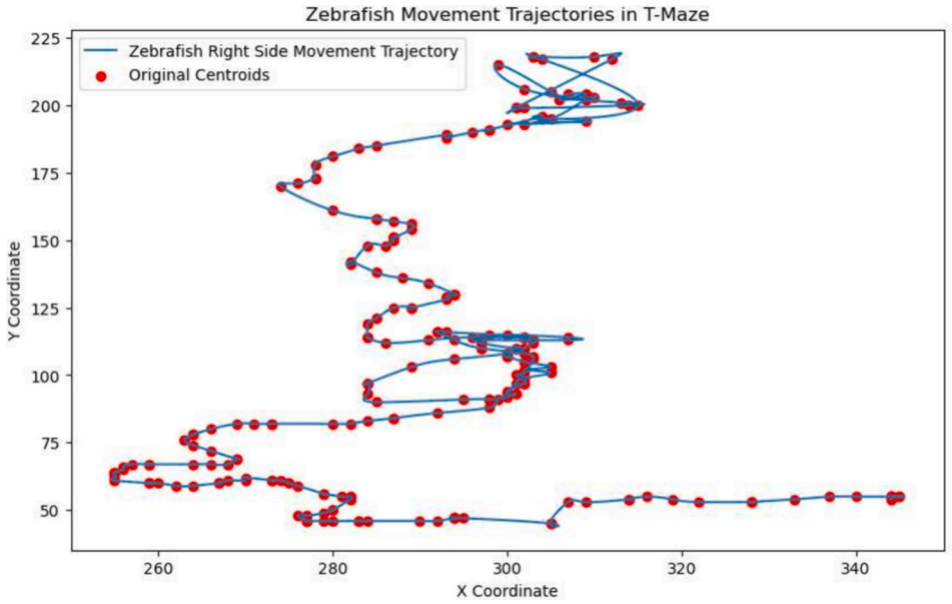

Fig. 6. Right movement.

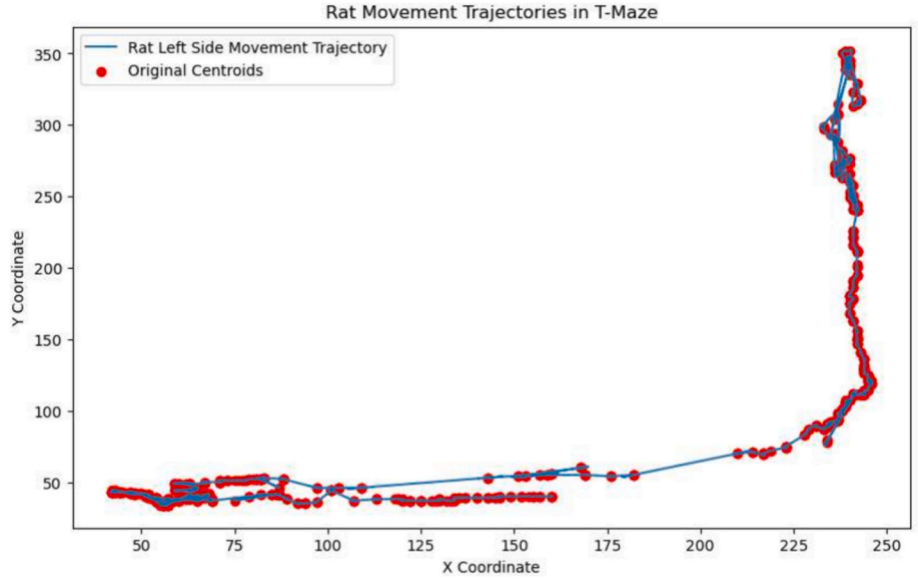

Fig. 7. Left movement.

search to ascertain the configuration that minimizes cross-validation error, thereby enhancing model precision.
- The selection of the distance metric, typically Euclidean, was predicated on the data's characteristics and the specific analytical prerequisites.

2. For SVM
   - The regularization parameter ('C') and the kernel type (linear) were calibrated through a synergistic application of grid search and cross-validation, aiming to mediate the balance between model complexity and its generalization prowess.
   - In instances involving non-linear SVMs, the kernel coefficient ('gamma') underwent optimization via grid search, ensuring the model's attunement to the data distribution.
3. For PCA-SVM
   - Commencing with dimensionality reduction via Principal Component Analysis (PCA), the number of components preserved was dictated by the explained variance ratio, to ensure the distilled dataset retained the majority of the original data's variance.
   - The SVM model was thereafter trained on this dimensionally reduced dataset, with hyperparameters refined as delineated above.

5.3.2. *Performance indicators*

To rigorously evaluate the efficacy of the proposed models in classifying animal behaviors within the T-maze, we implemented five key evaluation metrics: Precision, Recall, F1-score, Accuracy, and the Confusion Matrix. In this context, True Positives (*TP*) and True Negatives (*TN*) represent instances where the models correctly identified the behavior as the expected or alternative action. Conversely, False Positives (*FP*) and False Negatives (*FN*) reflect misclassifications that represent a potential misunderstanding of the animal's decision-making process. Accuracy, a cornerstone metric, is calculated by dividing the sum of correct classifications (*TP* and *TN*) by the total number of

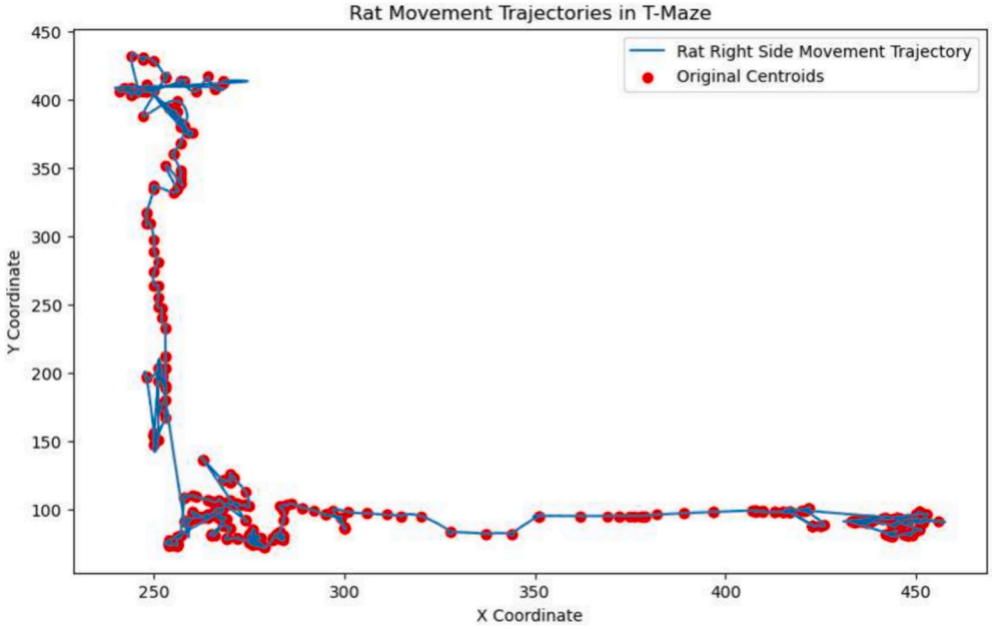

Fig. 8. Right movement.

observed behaviors, providing a holistic measure of the model's overall performance in capturing the complexities of animal cognitive behavior in the experimental setup.

The evaluation matrices are shown in the following equations:

$$\text{Recall} = \frac{FP}{(FP + TN)} \tag{5.1}$$

$$\text{Precision} = \frac{TP}{(TP + FP)} \tag{5.2}$$

$$\text{F1–score} = \frac{(2 \times TP)}{(2TP + FP + FN)} \tag{5.3}$$

$$\text{Accuracy} = \frac{(TP + TN)}{(TP + TN + FP + FN)} \tag{5.4}$$

5.3.3. Results analysis and comparison

The integration of K-Nearest Neighbors (KNN) and Support Vector Machine (SVM) classification algorithms (see (Bansal et al., 2022; Boateng et al., 2020)), along with a Principal Component Analysis-Support Vector Machine (PCA-SVM) hybrid approach (Hai and An, 2016), has significantly enhanced our understanding of zebrafish and rat movements within T-maze environments. This comprehensive analysis, as detailed in Tables 3 and 4, showcases the detailed insights gained from these methodologies. For zebrafish, the KNN model demonstrated high precision and recall in identifying left movements, with impressive metrics indicating its efficacy in minimizing false positives. Conversely, the SVM method outperformed in precision and recall for left movements, suggesting high accuracy in distinguishing them. Notably, by reducing dimensionality before classification, the PCA-SVM approach achieved remarkable accuracy rates of 98.07% for zebrafish and 98.15% for rats, highlighting its exceptional capability in interpreting complex behavioral data with minimal error.

Table 3
Comparative analysis of KNN, SVM, and PCA-SVM performance in classifying the left-right movements of zebrafish.

Method	Behavior	Precision %	Recall %	F-measure %	Accuracy %
KNN	Left Movement	96.92	96.91	95.63	96.11
	Right Movement	94.73	93.22	92.14	
SVM	Left Movement	98.43	96.92	97.67	97.08
	Right Movement	94.87	97.36	96.10	
PCA-SVM	Left Movement	96.87	98.92	98.41	98.07
	Right Movement	99.36	95.23	97.56	

Table 4
Comparative analysis of KNN, SVM, and PCA-SVM performance in classifying the left-right movements of rats.

Method	Behavior	Precision %	Recall %	F-measure %	Accuracy %
KNN	Left Movement	92.32	97.16	94.68	93.42
	Right Movement	95.32	87.74	91.37	
SVM	Left Movement	96.25	97.67	96.95	96.18
	Right Movement	96.07	93.72	94.88	
PCA-SVM	Left Movement	97.29	98.67	98.63	98.15
	Right Movement	98.07	94.59	97.22	

The PCA-SVM's standout performance is attributed to its ability to distill essential features from the behavioral data, enhancing the SVM's classification accuracy. This method's success underscores the potential of combining dimensionality reduction with machine learning algorithms to tackle the intricacies of animal behavior analysis. The detailed performance measures, including precision, recall, F-measure, and overall accuracy, affirm the robustness of PCA-SVM in capturing the behavior of animal movements within a controlled environment. This approach advances our understanding of animal cognition and exemplifies the transformative impact of machine learning techniques in behavioral science research.

The confusion matrices for the KNN and SVM classification methods and their PCA-enhanced versions reveal detailed insights into the models' classification capabilities for zebrafish and rat movements in a T-maze (see Figs. 9–14). For zebrafish, the SVM classifier demonstrates high accuracy and precision, with the PCA-SVM model further enhancing the true positive rates for both left and right movements while minimizing false positives, as shown in Figs. 10 and 11. The KNN

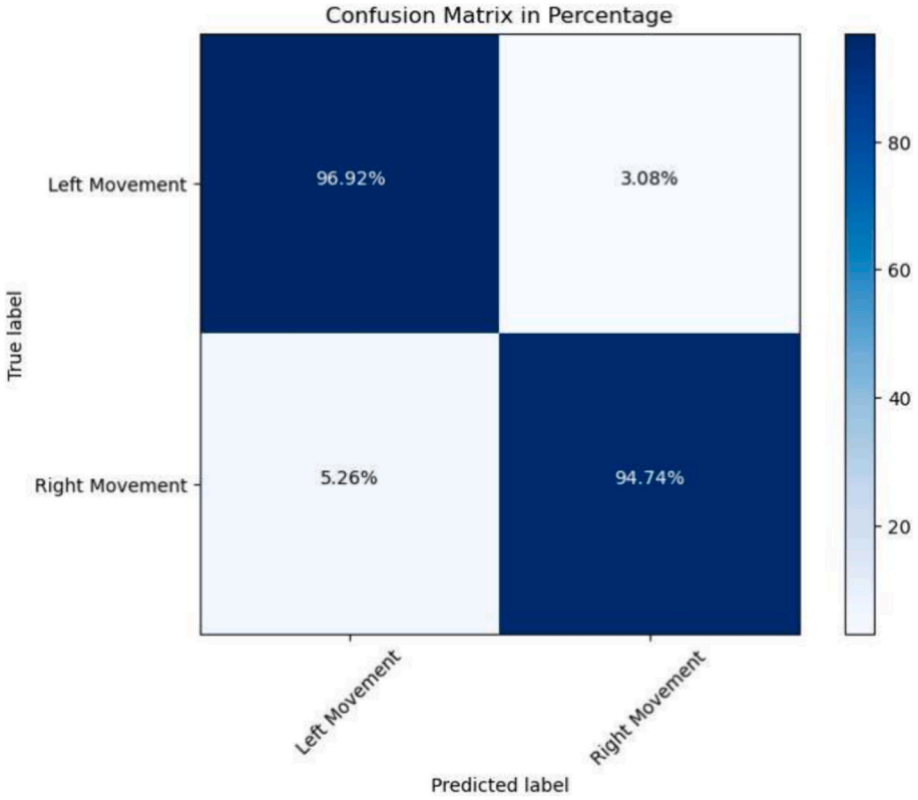

Fig. 9. KNN confusion matrix for zebrafish behavior.

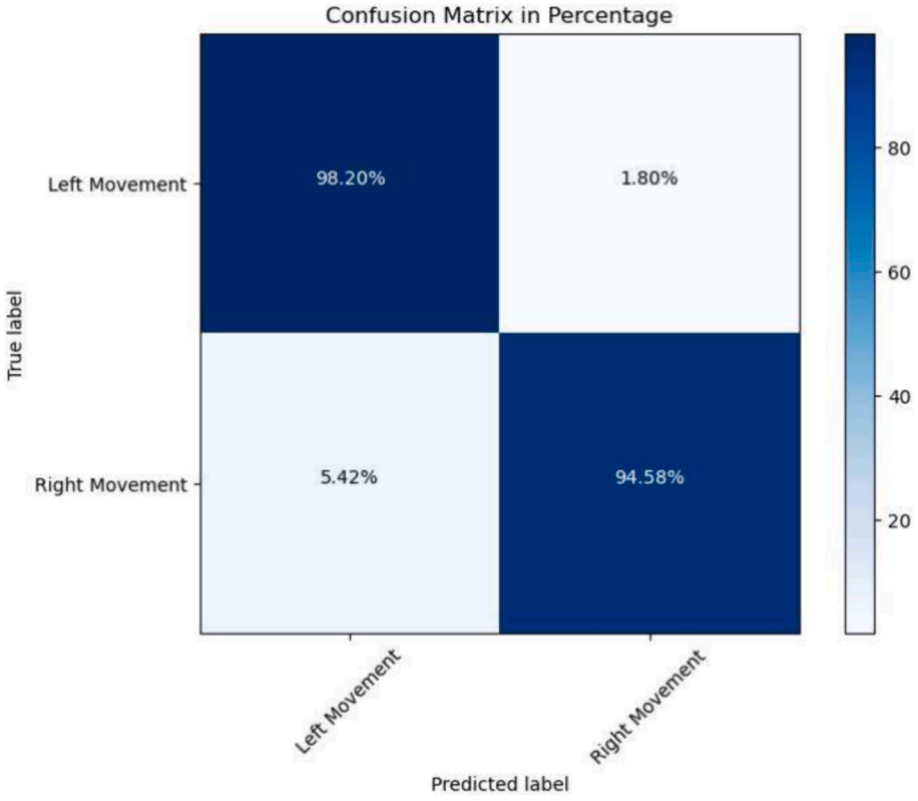

Fig. 10. SVM confusion matrix for zebrafish behavior.

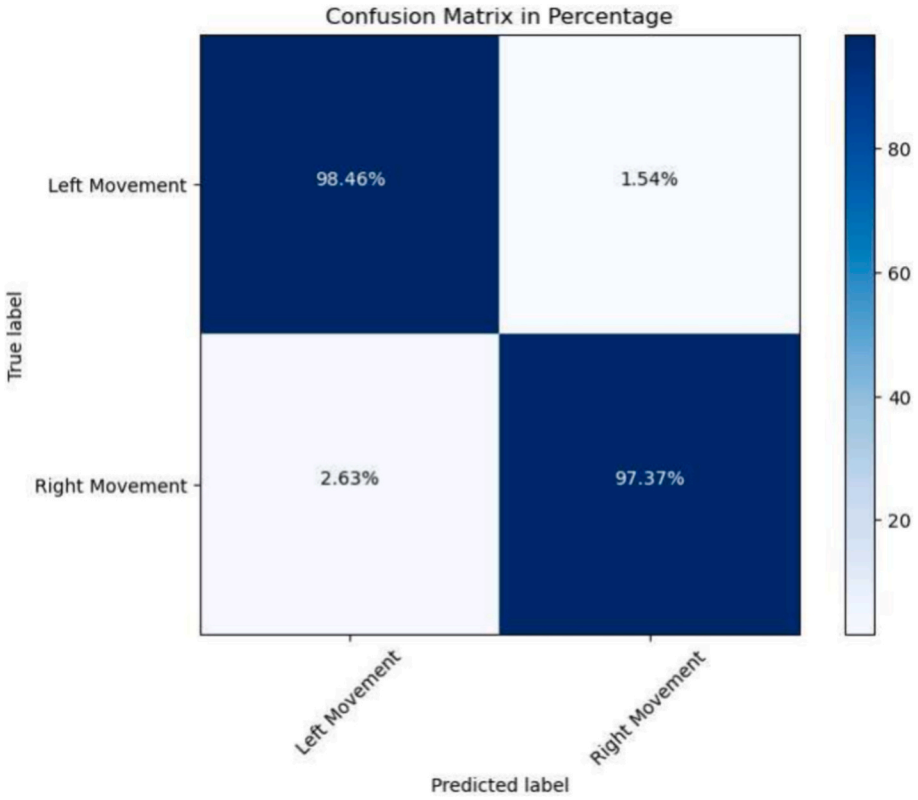

Fig. 11. PCA-SVM confusion matrix for zebrafish behavior.

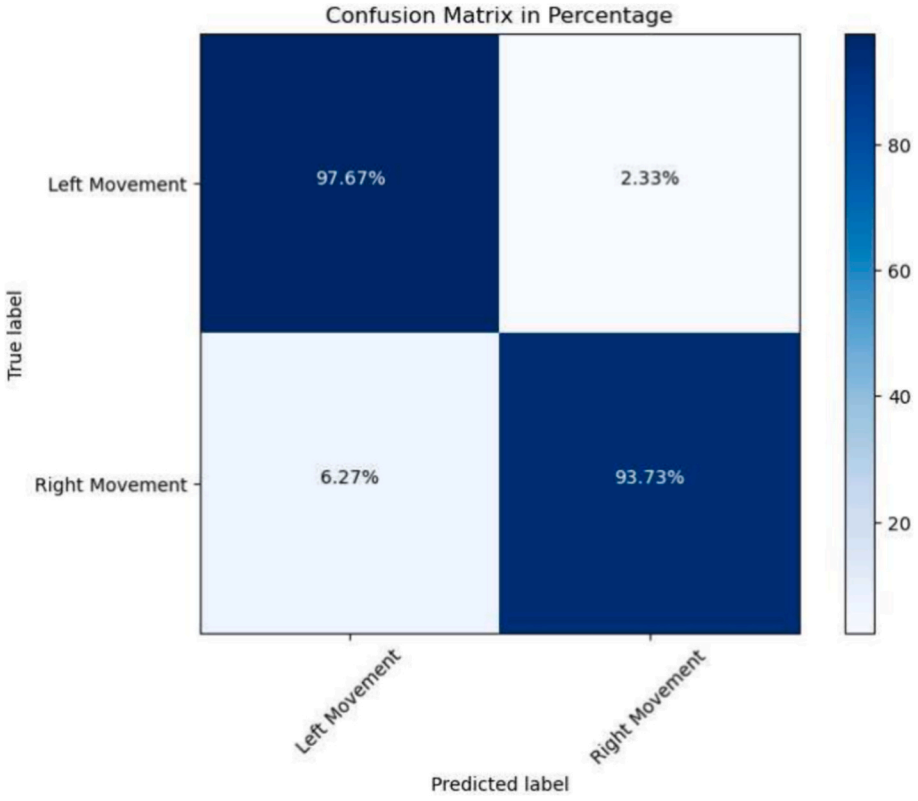

Fig. 12. KNN confusion matrix for rat behavior.

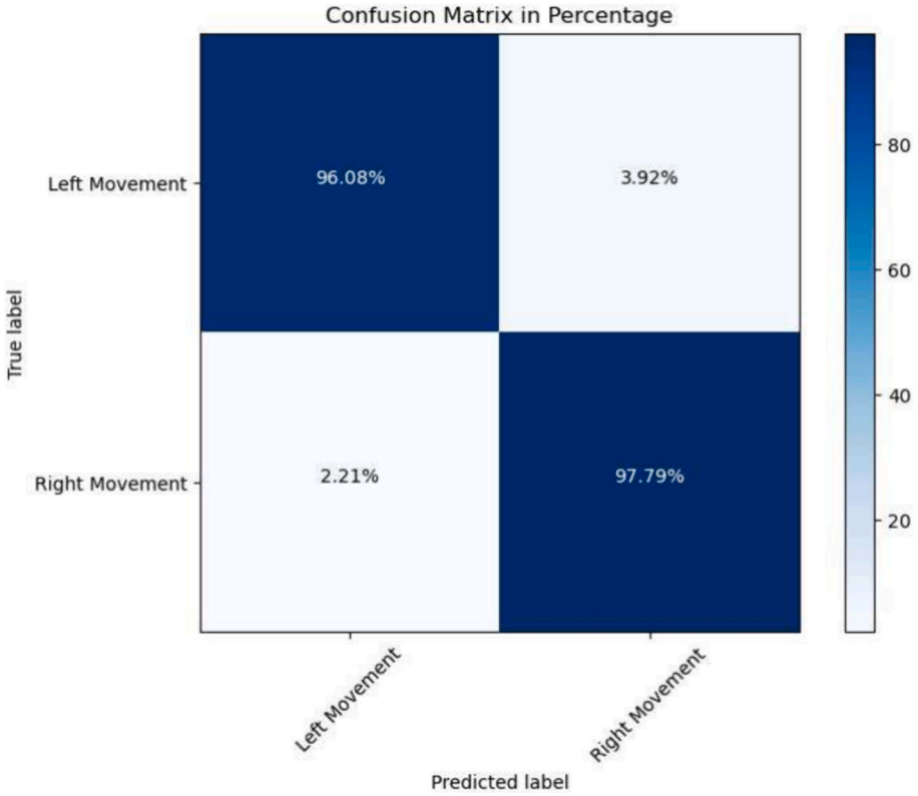

Fig. 13. SVM confusion matrix for rat behavior.

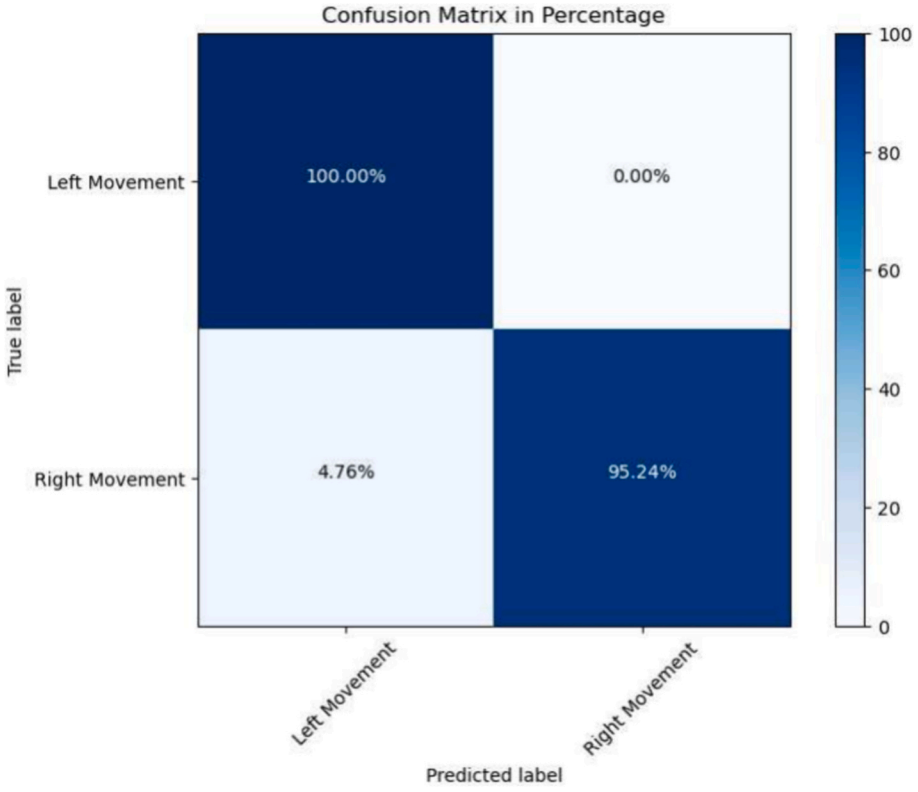

Fig. 14. PCA-SVM confusion matrix for rat behavior.

classifier, while slightly less precise, still maintains a high accuracy for zebrafish, as evidenced by Fig. 9, indicating its effectiveness in distinguishing the species' subtle movement variations.

The KNN classifier exhibits impressive precision in analyzing rat movements, possibly surpassing the standard SVM (Fig. 12). This might be attributed to its suitability for handling consistent and defined rat movement patterns. The PCA-SVM model for rats, illustrated in Fig. 14, achieves a perfect classification rate for left movements and a substantial accuracy for right movements, asserting its exceptional performance in processing rat behavioral data. Conversely, the SVM model displays a slight dip in precision for rat movements compared to zebrafish, as shown in Fig. 13, which might reflect the distinct challenges posed by the rats' movement dynamics.

These confusion matrices are pivotal for assessing the predictive prowess of each classification approach. By dissecting the true positive, false positive, true negative, and false negative rates, we understand the model's capability to distinguish left and right movements in zebrafish and rats accurately. Such a detailed evaluation not only delineates the comparative strengths and weaknesses of the classifiers but also enhances our comprehension of the behavioral patterns exhibited by these species in a structured experimental setup.

6. Conclusion

This study represents a significant advancement in understanding the complex decision-making processes of animals within T-maze environments, achieved through the integration of mathematical modeling and advanced machine-learning techniques. Beginning with the pioneering work of Bush and Wilson, (1956) on paradise fish, we developed a mathematical model to capture this behavioral phenomenon, establishing the existence, convergence, and stability of a unique solution. Our analysis, employing K-Nearest Neighbors (KNN), Support Vector Machine (SVM), and a hybrid approach of Principal Component Analysis (PCA) with SVM algorithms for zebrafish and rats, reveals intricate behavioral patterns. Notably, the PCA-SVM method demonstrated remarkable accuracy, achieving 98.07% for zebrafish and 98.15% for rats. This research advances our understanding of animal cognition. It underscores the potential of machine learning in behavioral science, setting the stage for further studies across a broader spectrum of species and decision-making contexts.

CRediT authorship contribution statement

Ali Turab: Writing – original draft, Validation, Project administration, Methodology, Funding acquisition, Formal analysis, Conceptualization. **Wutiphol Sintunavarat:** Visualization, Supervision, Methodology, Investigation, Formal analysis, Conceptualization. **Farhan Ullah:** Software, Resources, Methodology, Investigation, Data curation, Conceptualization. **Shujaat Ali Zaidi:** Visualization, Validation, Project administration, Investigation, Data curation, Conceptualization. **Andrés Montoyo:** Validation, Software, Formal analysis, Data curation, Conceptualization. **Josué-Antonio Nescolarde-Selva:** Writing – original draft, Validation, Software, Methodology, Investigation, Funding acquisition, Data curation.

Declaration of competing interest

The authors report no declarations of interest.

Data availability

Data will be made available on request.

Acknowledgements

This research is supported by the University of Alicante, Spain, the Spanish Ministry of Science and Innovation, the Generalitat Valenciana, Spain, and the European Regional Development Fund (ERDF) through the following funding: At the national level, the following projects were granted: TRIVIAL (PID2021-122263OB-C22); and CORTEX (PID2021-123956OB-I00), funded by MCIN/AEI/10.13039/501100011033 and, as appropriate, by "ERDF A way of making Europe", by the "European Union" or by the "European Union NextGenerationEU/PRTR". At regional level, the Generalitat Valenciana (Conselleria d'Educacio, Investigacio, Cultura i Esport), Spain, granted funding for NL4DISMIS (CIPROM/2021/21). This project is also funded by National Research Council of Thailand (NRCT) N41A640092.

References

Alvarez, A.M., 2021. Comparison of proxies for fish stock. A Monte Carlo analysis. Fish. Res. 238, 105901.
Aoki, T., 1950. On the stability of the linear transformation in Banach spaces. J. Math. Society Japan 2 (1–2), 64–66.
Balázsi, G., Van Oudenaarden, A., Collins, J.J., 2011. Cellular decision making and biological noise: from microbes to mammals. Cell 144 (6), 910–925.
Banach, S., 1922. Sur les opérations dans les ensembles abstraits et leur application aux équations intégrales. Fundam. Math. 3 (1), 133–181.
Bansal, M., Goyal, A., Choudhary, A., 2022. A comparative analysis of K-nearest neighbor, genetic, support vector machine, decision tree, and long short term memory algorithms in machine learning. Decision Anal. J. 3, 100071.
Barak, O., Tsodyks, M., 2023. Mathematical models of learning and what can be learned from them. Curr. Opin. Neurobiol. 80, 102721.
Benvenutti, R., Marcon, M., Gallas-Lopes, M., de Mello, A.J., Herrmann, A.P., Piato, A., 2021. Swimming in the maze: An overview of maze apparatuses and protocols to assess zebrafish behavior. Neurosci. Biobehav. Rev. 127, 761–778.
Berinde, V., Takens, F., 2007. Iterative Approximation of Fixed Points (Vol. 1912, Pp. Xvi +−322). Springer, Berlin.
Bhattacharjee, S., MacPherson, B., Wang, R.F., Gras, R., 2019. Animal communication of fear and safety related to foraging behavior and fitness: An individual-based modeling approach. Eco. Inform. 54, 101011.
Bleuven, C., Landry, C.R., 2016. Molecular and cellular bases of adaptation to a changing environment in microorganisms. Proc. R. Soc. B Biol. Sci. 283 (1841), 20161458.
Boateng, E.Y., Otoo, J., Abaye, D.A., 2020. Basic tenets of classification algorithms K-nearest-neighbor, support vector machine, random forest and neural network: a review. J. Data Anal. Inform. Proc. 8 (4), 341–357.
Browning, E., Bolton, M., Owen, E., Shoji, A., Guilford, T., Freeman, R., 2018. Predicting animal behaviour using deep learning: GPS data alone accurately predict diving in seabirds. Methods Ecol. Evol. 9 (3), 681–692.
Bush, R.R., Wilson, T.R., 1956. Two-choice behavior of paradise fish. J. Exp. Psychol. 51 (5), 315.
Calenge, C., Dray, S., Royer-Carenzi, M., 2009. The concept of animals' trajectories from a data analysis perspective. Eco. Inform. 4 (1), 34–41.
Cognato, G.D.P., Bortolotto, J.W., Blazina, A.R., Christoff, R.R., Lara, D.R., Vianna, M.R., Bonan, C.D., 2012. Y-maze memory task in zebrafish (Danio rerio): the role of glutamatergic and cholinergic systems on the acquisition and consolidation periods. Neurobiol. Learn. Mem. 98 (4), 321–328.
Collins, A.G., Shenhav, A., 2022. Advances in modeling learning and decision-making in neuroscience. Neuropsychopharmacology 47 (1), 104–118.
Deacon, R.M., Rawlins, J.N.P., 2006a. T-maze alternation in the rodent. Nat. Protoc. 1 (1), 7–12.
Deacon, R.M., Rawlins, J.N.P., 2006b. T-maze alternation in the rodent. Nat. Protoc. 1 (1), 7–12.
Debnath, P., 2021. A mathematical model using fixed point theorem for two-choice behavior of rhesus monkeys in a noncontingent environment. Metric Fixed Point Theory: Appl. Sci. Eng. Behav. Sci. 345–353.
Dember, W.N., Kleinman, R., 1973. Cues for spontaneous alternation by gerbils. Anim. Learn. Behav. 1 (4), 287–289.
Dember, W.N., Richman, C.L. (Eds.), 2012. Spontaneous Alternation Behavior. Springer Science & Business Media.
Dennis, W., 1935. A comparison of the rat's first and second explorations of a maze unit. Am. J. Psychol. 47 (3), 488–490.
Dennis, W., 1939. Spontaneous alternation in rats as an indicator of the persistence of stimulus effects. J. Comp. Psychol. 28 (2), 305.
Dennis, W., Henneman, R.H., 1932. The non-random character of initial maze behavior. Pedagog. Seminary J. Genet. Psychol. 40 (2), 396–405.
Dennis, W., Sollenberger, R.T., 1934. Negative adaptation in the maze exploration of albino rats. J. Comp. Psychol. 18 (2), 197.
d'Isa, R., Comi, G., Leocani, L., 2021. Apparatus design and behavioural testing protocol for the evaluation of spatial working memory in mice through the spontaneous alternation T-maze. Sci. Rep. 11 (1), 21177.
Dixon, M., Polson, N., 2020. Deep fundamental factor models. SIAM J. Financ. Math. 11 (3), SC26-SC37.
Douglas, R.J., Peterson, J.J., Douglas, D.P., 1973. The ontogeny of a hippocampus-dependent response in two rodent species. Behav. Biol. 8 (1), 27–37.
Epstein, B., 1966. On a difference equation arising in a learning-theory model. Israel J. Math. 4 (3), 145–152.

Ferrarini, A., Gustin, M., 2022. Introducing a new tool to derive animal behaviour from GPS data without ancillary data: the red-footed falcon in Italy as a case study. Eco. Inform. 69, 101645.
Fidura, F.G., Leberer, M.R., 1974. Spontaneous alternation as a function of number of forced-choice responses in the goldfish (Carassius auratus). Bull. Psychon. Soc. 3 (3), 181–182.
Frederickson, C.J., Frederickson, M.H., 1979. Emergence of spontaneous alternation in the kitten. Develop. Psychobiol. J. Int. Soc. Develop. Psychobiol. 12 (6), 615–621.
George, R., Mitrović, Z.D., Turab, A., Savić, A., Ali, W., 2022. On a unique solution of a class of stochastic predator–prey models with two-choice behavior of predator animals. Symmetry 14 (5), 846.
Hai, N.T., An, T.H., 2016. PCA-SVM algorithm for classification of skeletal data-based eigen postures. Am. J. Biomed. Eng 6, 47–158.
Henderson, N.D., 1970. A genetic analysis of spontaneous alternation in mice. Behav. Genet. 1 (2), 125–132.
Hughes, R.N., 1965. Spontaneous alteration and response to stimulus change in the ferret. J. Comp. Physiol. Psychol. 60 (1), 149.
Hughes, R.N., 1967. Turn alternation in woodlice (Porcellio scaber). Anim. Behav. 15 (2–3), 282–286.
Hughes, R.N., 1973. Spontaneous alternation in adult rabbits. Bull. Psychon. Soc. 2 (1), 2.
Hyers, D.H., 1941. On the stability of the linear functional equation. Proc. Natl. Acad. Sci. 27 (4), 222–224.
Hyers, D.H., Isac, G., Rassias, T., 2012. Stability of Functional Equations in Several Variables, vol. 34. Springer Science & Business Media.
Ishikawa, S., 1974. Fixed points by a new iteration method. Proc. Am. Math. Soc. 44 (1), 147–150.
Istrăţescu, V.I., 1976. On a functional equation. J. Math. Anal. Appl. 56 (1), 133–136.
Izumi, A., Tsuchida, J., Yamaguchi, C., 2013. Spontaneous alternation behavior in common marmosets (Callithrix jacchus). J. Comp. Psychol. 127 (1), 76.
Johnson, A., Redish, A.D., 2007. Neural ensembles in CA3 transiently encode paths forward of the animal at a decision point. J. Neurosci. 27 (45), 12176–12189.
Kirkby, R.J., Lackey, G.H., 1968. Spontaneous alternation in Mesocricetus auratus: age differences. Psychon. Sci. 10 (7), 257–258.
Kliegr, T., Bahník, Š., Fürnkranz, J., 2020. Advances in machine learning for the behavioral sciences. Am. Behav. Sci. 64 (2), 145–175.
Kuru, K., Clough, S., Ansell, D., McCarthy, J., McGovern, S., 2023. Intelligent airborne monitoring of irregularly shaped man-made marine objects using statistical machine learning techniques. Eco. Inform. 78, 102285.
Lewis, S.A., Negelspach, D.C., Kaladchibachi, S., Cowen, S.L., Fernandez, F., 2017. Spontaneous alternation: a potential gateway to spatial working memory in Drosophila. Neurobiol. Learn. Mem. 142, 230–235.
Liu, X., Gao, J., Liu, Y., Zheng, N., Liu, R., 2023, September. Motion-scenario decoupling for rat-aware video position prediction: Strategy and benchmark. In: International Conference on Image and Graphics. Springer Nature Switzerland, Cham, pp. 136–148.
Lucon-Xiccato, T., Bisazza, A., 2017. Complex maze learning by fish. Anim. Behav. 125, 69–75.
Lyon, P., 2015. The cognitive cell: bacterial behavior reconsidered. Front. Microbiol. 6, 119153.
Mann, W.R., 1953. Mean value methods in iteration. Proc. Am. Math. Soc. 4 (3), 506–510.
Marar, H.W., 2024. Advancements in software engineering using AI. Comp. Software Media App. 6 (1), 3906.
May, R.B., Wellman, A.W., 1968. Alternation in the fruit fly, Drosophila melanogaster. Psychonomic. Science 12 (7), 339–340.
Montgomery, K.C., 1952. Exploratory behavior and its relation to spontaneous alternation in a series of maze exposures. J. Comp. Physiol. Psychol. 45 (1), 50.
Nazir, S., Kaleem, M., 2021. Advances in image acquisition and processing technologies transforming animal ecological studies. Eco. Inform. 61, 101212.
Okeke, G.A., Abbas, M., 2017. A solution of delay differential equations via Picard–Krasnoselskii hybrid iterative process. Arab. J. Math. 6, 21–29.
Picard, É., 1890. Memoire sur la theorie des equations aux derivees partielles et la methode des approximations successives. J. Math. pures appl. 6, 145–210.
Preuschoff, K., Mohr, P.N., Hsu, M., 2013. Decision making under uncertainty. Front. Neurosci. 7, 72771.
Ramey, P.A., Teichman, E., Oleksiak, J., Balci, F., 2009. Spontaneous alternation in marine crabs: invasive versus native species. Behav. Process. 82 (1), 51–55.
Rassias, T.M., 1978. On the stability of the linear mapping in Banach spaces. Proc. Am. Math. Soc. 72 (2), 297–300.
Schein, E.H., 1954. The effect of reward on adult imitative behavior. J. Abnorm. Soc. Psychol. 49 (3), 389.
Shokaku, T., Moriyama, T., Murakami, H., Shinohara, S., Manome, N., Morioka, K., 2020. Development of an automatic turntable-type multiple T-maze device and observation of pill bug behavior. Rev. Sci. Instrum. 91 (10).
Sih, A., Bell, A.M., Johnson, J.C., Ziemba, R.E., 2004. Behavioral syndromes: an integrative overview. Q. Rev. Biol. 79 (3), 241–277.
Tilley, M.W., Doolittle, J.H., Mason, D.J., 1966. Spontaneous alternation in the Virginia opossum. Psychol. Rep. 19 (2), 593–594.
Tolman, E.C., 1925. Purpose and cognition: the determiners of animal learning. Psychol. Rev. 32 (4), 285.
Tolman, E.C., 1948. Cognitive maps in rats and men. Psychol. Rev. 55 (4), 189.
Tron, E., Margaliot, M., 2004. Mathematical modeling of observed natural behavior: a fuzzy logic approach. Fuzzy Sets Syst. 146 (3), 437–450.
Turab, A., Sintunavarat, W., 2019. On analytic model for two-choice behavior of the paradise fish based on the fixed point method. J. fixed point theory appl. 21, 1–13.
Turab, A., Sintunavarat, W., 2020. On the solution of the traumatic avoidance learning model approached by the Banach fixed point theorem. J. fixed point theory appl. 22, 1–12.
Turab, A., Sintunavarat, W., 2023. On the solution of the generalized functional equation arising in mathematical psychology and theory of learning approached by the Banach fixed point theorem. Carpathian J. Math. 39 (2), 541–551.
Turab, A., Mlaiki, N., Fatima, N., Mitrović, Z.D., Ali, W., 2022a. Analysis of a class of stochastic animal behavior models under specific choice preferences. Mathematics 10 (12), 1975.
Turab, A., Brzdek, J., Ali, W., 2022b. On solutions and stability of stochastic functional equations emerging in psychological theory of learning. Axioms 11 (3), 143.
Turab, A., Rosli, N., Ali, W., Nieto, J.J., 2023. The existence and uniqueness of solutions to a functional equation arising in psychological learning theory. Demonst. Math. 56 (1), 20220231.
Ulam, S.M., 2012. A collection of the mathematical problems. Interscience Publ, New York, 1960. Received: September.
Valletta, J.J., Torney, C., Kings, M., Thornton, A., Madden, J., 2017. Applications of machine learning in animal behaviour studies. Anim. Behav. 124, 203–220.
Vos, M., Vet, L.E., Wäckers, F.L., Middelburg, J.J., Van Der Putten, W.H., Mooij, W.M., Van Donk, E., 2006. Infochemicals structure marine, terrestrial and freshwater food webs: implications for ecological informatics. Eco. Inform. 1 (1), 23–32.
Wang, G., 2019. Machine learning for inferring animal behavior from location and movement data. Eco. Inform. 49, 69–76.
Xiang, T., Yuan, R., 2015. A note on Krasnosel'skii fixed point theorem. Fixed Point Theory Appl. 2015, 1–8.
Xiao, Y., Segal, M.R., 2009. Identification of yeast transcriptional regulation networks using multivariate random forests. PLoS Comput. Biol. 5 (6), e1000414.
Yang, Y., Mailman, R.B., 2018. Strategic neuronal encoding in medial prefrontal cortex of spatial working memory in the T-maze. Behav. Brain Res. 343, 50–60.
Yerkes, R.M., 1912. The intelligence of earthworms. J. Anim. Behav. 2 (5), 332.
Zhang, X., Zou, J., He, K., Sun, J., 2015. Accelerating very deep convolutional networks for classification and detection. IEEE Trans. Pattern Anal. Mach. Intell. 38 (10), 1943–1955.